BioID indicates the involvement of the TRAPP protein TrappC11 in autophagy

Qingchuan Zhao

A Thesis

in

The Department

of

Biology

Presented in Partial Fulfillment of the Requirements

for the Degree of Master of Science (Biology) at

Concordia University

Montreal, Quebec, Canada

October 2016

CONCORDIA UNIVERSITY

School of Graduate Studies

This is to certify that the thesis prepared

By: Qingchuan Zhao

Entitled: BioID indicates the involvement of the TRAPP protein TrappC11 in autophagy

and submitted in partial fulfillment of the requirements for the degree of

Master of Science (Biology)

complies with the regulations of the University and meets the accepted standards with respect to originality and quality.

Signed by the final Examining Committee:

_____Chair
Dr. G. Brown

_____Examiner
Dr. A. Piekny

_____Examiner
Dr. M. Whiteway

_____Examiner
Dr. V. Titorenko

_____Supervisor
Dr. M. Sacher

Approved by _____
Dr. G. Brown (Graduate Program Director)

_____
Dr. A. Roy (Dean of Faculty of Arts and Science)

Date _____November 21st, 2016_____

ABSTRACT

BioID indicates the involvement of the TRAPP protein TrappC11 in autophagy

Qingchuan Zhao

The Transport protein particle (TRAPP) complexes are molecular machines that function in various membrane transport processes including the secretory pathway. Recently, one form of the TRAPP complex, TRAPPIII, has been shown to be involved in autophagy, a cellular recycling process that delivers cytoplasmic components to lysosomes for degradation. Mutations in TrappC11, one subunit in TRAPPIII, have been reported to be associated with muscular dystrophy and intellectual disability. To understand mutated TrappC11 could lead to the phenotypes, I employed BioID to identify TrappC11 interacting proteins. To perform BioID, I constructed TrappC11 fused to BirA*, a biotin ligase that catalyzes the biotinylation of proteins within proximity to the fusion protein. The biotinylated proteins were then isolated and identified by mass spectrometry. The BioID approach revealed the autophagy-related proteins Atg2A, Atg2B, WDR45, p62/SQSTM1, and NBR1 as potential TrappC11 interacting partners, suggesting the involvement of TrappC11 in autophagy. Consistently, transient and stable knockdown of TrappC11 in HeLa cells both resulted in an accumulation of autophagosomes in non-starved cells as well as an increase of cellular lipid droplets. The distribution of lysosomes was also effected by the TrappC11 knockdown. Moreover, expression of eGFP-TrappC11 resulted in the formation of cytoplasmic puncta that partially overlapped with p62/SQSTM1, consistent with the BioID data that suggested an interaction between TrappC11 and this selective autophagy receptor. Taken together, my data indicate that TrappC11 might have an important role in non-starvation induced autophagy.

ACKNOWLEDGEMENTS

TABLE OF CONTENTS

LIST OF FIGURES

LIST OF TABLES

LIST OF ABBREVIATIONS

Adipose triglyceride lipase	ATGL
Autophagy-related genes	Atg
Blocked early in transport 3/5	Bet3/5
Bovine serum albumin	BSA
Chaperone-mediated autophagy	CMA
Clustered regularly interspaced short palindromic repeats	CRISPR
Coat protein II	COP II
Dimethyl sulfoxide	DMSO
Dithiothreitol	DTT
Dulbecco's modified eagle medium	DMEM
Endoplasmic reticulum	ER
ER-Golgi intermediate compartment	ERGIC
Ethylenediaminetetraacetic acid	EDTA
Fetal bovine serum	FBS
Gamma-aminobutyric receptor-associated protein	GABARAP
Golgi apparatus	Golgi
Green fluorescent protein	GFP
Gtpase activating protein	GAP
Guanine nucleotide exchange factor	GEF
Guanosine-5'-triphosphate	GTP
Heat shock 70 kda protein	Hsc70
Homotypic fusion and vacuole protein sorting	HOPS
Lipid droplet	LD
LC3-interacting regions	LIR
Lysosomal membrane proteins 1/2	LAMP1/2
Mechanistic target of rapamycin complex 1	mTORC1
Microtubule-associated protein 1light chain 3 protein	LC3
Multisubunit tethering complexe	MTC
Paraformaldehyde	PFA

Perilipin	PLIN
Phosphate buffered saline	PBS
Phosphatidylethanolamine	PE
Phosphatidylinositol 3-phosphate	PtdIns3P (PI3P)
Phosphotidylinositol 3-kinase	PI3K
Polymerase chain reaction	PCR
Pre-autophagosomal structure	PAS
SDS polyacrylamide electrophoresis	SDS-PAGE
Small interfering RNA	siRNA
Small Rab gtpase	Rab
Sodium dodecyl sulfate	SDS
Soluble N-ethylmaleimide-sensitive factor Attachment protein receptors	SNARE
Spondyloepiphyseal dysplasia tarda	SEDT
Syntaxin 17	STX17
Target-localized SNARE protein	t-SNARE
Tetratricopeptide repeat	TPR
Trafficking protein particle complex 11	TrappC11
Transport protein particle	TRAPP
TRAPP subunit 23/31	Trs23/31
Ubiquitin binding domains	UBD
Unfolded protein response	UPR
UV radiation resistance-associated gene	UVRAG
Vesicle-associated membrane protein 8	VAMP-8
Vesicle-localized SNARE protein	v-SNARE

Chapter 1: Introduction

1.1 Membrane trafficking, tethering and TRAPP

Eukaryotic cells are characterized by an endomembrane network system composed of different organelles, such as endoplasmic reticulum, Golgi, endosomes and lysosomes. The movement of materials between different organelles and membrane components is described as membrane trafficking (Bröcker et al., 2010; Chia and Gleeson, 2014). During this process, membrane-bound transport vesicles serve as shuttles which bud from a donor membrane and subsequently fuse to a particular recipient organelle. The core regulators of fusion are soluble N-ethylmaleimide-sensitive factor attachment protein receptors (SNAREs) (Jahn and Scheller, 2006). There are two complementary subsets of SNAREs localized on each set of membranes, with v-SNAREs on the vesicle membrane and t-SNAREs on the target membrane. The high stability of the SNARE complex overcomes the energy barrier to promote the membrane fusion between vesicle and target membrane, which allows the cargo to enter the target organelle (Weber et al., 1998; Dubuke and Munson, 2016). However, due to the limited functional distance caused by their small size, SNAREs can only regulate a very late stage of the vesicle-target membrane recognition process (Spang, 2016). The control of specificity of membrane fusion requires other protein families such as the Sec1/Munc18 proteins and the tethering factors, which are properly localized at each site of fusion membranes (Morgera et al., 2012).

1.1.1 Tethering factors

Tethering factors are a group of extended proteins or protein complexes that function in membrane tethering, a process to grasp vesicles and establish the first interaction between vesicles and target membranes before fusion of the two lipid bilayers (Chia and Gleeson, 2014). Tethering factors are essential for the fidelity of membrane trafficking as well as for the efficient assembly of SNARE complexes between the vesicle membrane and target membrane. Lines of evidence showed that loss of function of tethering factors leads to a block of membrane transport and interrupt the organization and identity of compartments (Gillingham et al., 2004; Nakajima, 1991; Sztul, 2005).

Tethering factors can be categorized into two classes: coiled-coil tethers and multisubunit tethering complexes (MTCs) (Barrowman et al., 2010). Both classes are highly conserved in eukaryotic cells and can be found throughout the secretory and endosomal pathways. Coiled-coil tethers are large hydrophilic proteins that are composed of homodimers with globular heads and long coiled-coil domains (Chia and Gleeson, 2014). Due to their elongated nature, coiled-coil tethers can capture the incoming vesicles over long distances (of more than 200 nm), and create a relatively long-distance link between vesicle and target membrane (Bröcker et al., 2010). Unlike coiled-coil tethers, MTCs are thought to tether a captured vesicle in a close distance (up to 30 nm) to its target compartment and maintain its position for fusion (Yu and Hughson, 2010). Although MTCs differ in membrane trafficking pathways and composition of subunits, they share similarities in their interacting families of proteins: Rab guanosine triphosphatase (Rab GTPases), SM proteins, coat proteins, and SNAREs. In addition, some MTCs also interact with the particular guanine nucleotide exchange factor (GEF) for their GTPases (Dubuke and Munson, 2016).

1.1.2 TRAPP complex

Transport protein particle (TRAPP) complexes are one subset of MTCs, which interact with coat proteins and have tethering roles in both the secretory and endolysosomal pathways as well as functions in autophagy (Barrowman et al., 2010). However, TRAPPs are atypical tethering factors which share the least similarity with other MTCs in sequence and structure (Cai et al., 2008). Additionally, TRAPPs may function differently than other MTCs since they directly act as GEFs and no interaction has yet been shown between them and SNAREs or Sec1/Munc18 proteins (Dubuke and Munson, 2016; Sacher et al., 2001).

The identification of TRAPPs was done first in the yeast *Saccharomyces cerevisiae* (Sacher et al., 1998). Blocked early in transport 3 (Bet3) was the first identified TRAPP subunit. Subsequently, Bet3 co-immunoprecipitating proteins were identified and were revealed to compose three TRAPP complexes in yeast, namely TRAPP I, TRAPP II and TRAPP III (Barrowman et al., 2010). All three forms share common four core subunits, Bet3, Bet5, TRAPP subunit 23 (Trs23) and Trs31, which are required for activation of Ypt1, a small Rab GTPase required for fusion of ER-derived vesicles with the Golgi (Wang et. al, 2000; Kim et al., 2016). TRAPP I tethers COP II-coated vesicles during ER to Golgi traffic while TRAPP II functions during intra-Golgi transport (Sacher et al., 2001; Barrowman et al., 2010). Unlike the other two forms acting in the secretory pathway, TRAPP III has been shown to be required for membrane expansion during autophagy, a lysosomal degradation-based cellular recycling process (Lynch-Day et al., 2010).

TRAPP complexes are conserved from yeast to mammals. So far, two forms of TRAPPs have been isolated from mammalian cells, TRAPPII and TRAPPIII (Kim et al., 2016). Similar to

yeast TRAPPs, mammalian TRAPPs tether ER-derived vesicles to the Golgi and function as GEFs for Rab1, the mammalian homologue of Ypt1, which ultimately recruits SNAREs to mediate vesicle fusion with target membranes (Barrowman et al., 2010; Kim et al., 2016). Depletion of subunits TrappC3, TrappC8, TrappC11 and TrappC12 results in fragmentation of the Golgi apparatus and blocks ER-Golgi trafficking (Scrivens et al., 2011). As expected from the characteristics of the yeast TRAPP III, one component of mammalian TRAPP III (TRAPPC8) has recently, been shown to be involved in autophagy (Lamb et al., 2016). While similarities are shared between mammalian TRAPPs and yeast TRAPPs, significant differences cannot be ignored. Several mammalian TRAPP subunits have more than one isoform, and two additional subunits existing in mammalian TRAPP III, TrappC11 and TrappC12, are metazoan-specific (Kümmel et al., 2008; Scrivens et al., 2011).

Mutations of TRAPP subunits are broadly related to human diseases. Although being in the same complex, the diseases caused by mutations of different TRAPP subunits are dramatically divergent (Kim et al., 2016). Mutations in *TRAPPC2* are associated with X-linked spondyloepiphyseal dysplasia tarda (SEDT), a skeletal disease causing a short stature, a short trunk, a barrel-shaped chest and disproportionately long arms (Gedeon et al., 1999). TRAPPC4 mutation is related to colorectal carcinogenesis. The interaction between TrappC4 and ERK2 regulates cell proliferation and apoptosis in colorectal cancer cells (Zhao et al., 2011; Weng et al., 2014). TRAPPC6 mutation has been linked to Alzheimer's disease, as experiments show N-terminal internal deletion isoform of TrappC6A leads to Tau aggregation (Hamilton et al., 2011; Chang et al., 2015). TRAPPC9 mutation is associated with intellectual disability and schizophrenia (Mir et al., 2009; Mochida et al., 2009). Mutations of TRAPPC11 can cause muscular dystrophy and steatosis (see below for details) (Bögershausen et al., 2013; Liang et al., 2015). The lack of

overlapping effects of TRAPP subunit mutations suggests that individual subunits may play roles in cellular processes not related to TRAPP complex functions. In fact, a recent paper showing a moonlighting function of TrappC12 in mitosis supports the possibility of complex-independent functions (Milev et al., 2015).

1.1.3 Function of TrappC11 and its involvement in disease

In human cells, TrappC11 is a subunit of the TRAPPIII complex. Although a TRAPPC11 orthologue is not readily detected in yeast TRAPP complexes, it is highly conserved in metazoans (Kim et al., 2016). The human TrappC11 is a 130 kD protein with two highly conserved central domains; the foie gras and gryzun domains, and six tetratricopeptide repeat (TPR) domains, which are usually considered as protein interacting regions (Bögershausen et al., 2013; Brunet and Sacher, 2014). Some studies show TRAPPC11 is an essential gene. Flies homozygous for an allele that has an insertion in *gryzun* at residue 447 die at the end of embryogenesis (Wendler et al., 2010). Recent studies of human essential genes through genome-wide CRISPR-Cas9 screens indicated that TRAPPC11 is required for cell viability (Blomen et al., 2015; Hart et al., 2015; Shalem et al., 2014).

However, little has been known about functions of TrappC11. It is likely that TrappC11 functions at the Golgi. As a component of TRAPP III, TRAPPC11 is required for the integrity of the Golgi and disruption of TRAPPC11 causes Golgi fragmentation and vesiculation as shown in Drosophila (Wendler et al., 2010), zebrafish (DeRossi et al., 2016) and human cells (Scrivens et al., 2011). The scattered Golgi may be the result of an impaired ability of TrappC11 to bind other TRAPP subunits (Bögershausen et al., 2013). Although the localization of mammalian TRAPPC11

remains unknown, staining of gryzun, the Drosophila homologue of TRAPPC11, showed partial co-localization with the Golgi (Wendler et al., 2010). TrappC11 is also crucial for the secretory pathway, since trappc11-mutated zebrafish display secretory protein retention (DeRossi et al., 2016) and depletion of the protein by siRNA from cultured cells results in a block in post-ER trafficking (Scrivens et al., 2011; Wendler et al., 2010).

The importance of TRAPPC11 has also been shown in individuals and organisms carrying TRAPPC11 mutations. Drosophila *gryzun* mutants reveal defects in learning and memory (Dubnau et al., 2003); patients carrying *TRAPPC11* mutations suffer from limb girdle muscular dystrophy, intellectual disability and even hyperkinetic movements (Bögershausen et al., 2013). Recently, another patient with compound heterozygous mutations in *TRAPPC11* was reported having steatosis, infantile-onset cataract, and congenital muscular dystrophy (Liang et al., 2015). Similarly, zebrafish with *foie gras* (*fgr)* mutation developed fatty liver, defects in the visual system, as well as abnormal fins, smaller gut and jaw (Sadler et al., 2005). The *fgr/trappc11* fatty liver phenotype is considered as a result of activation of the unfolded protein response (Cinaroglu et al., 2011). A recent paper demonstrated that TRAPPC11 is required for protein N-glycosylation. Hypoglycosylated proteins are accumulated in *trappc11* mutated zebrafish, which leads to stressed UPR, and further causes fatty liver (DeRossi et al., 2016).

1.2 Autophagy

Autophagy is a cellular recycling process which delivers cytoplasmic components to lysosomes for degradation. This process is conserved in various types of cells from different organisms (Yang and Klionsky, 2009). According to the different mechanisms of lysosome cargo

delivery, autophagy can be categorized into three types: macroautophagy, chaperone-mediated autophagy (CMA), and microautophagy (Badadani, 2012). Macroautophagy, an in-bulk cargo degradation mechanism, requires the involvement of more than 30 autophagy proteins. These autophagy proteins regulate the formation of double-membrane autophagosomes and cargo delivery to lysosomes. In contrast, CMA only selectively degrades a single protein each time. In the CMA pathway, cytosolic heat shock cognate protein 70 (Hsc70) recognizes proteins bearing a pentapeptide motif (a KFERQ-like motif) and delivers the single protein to the lysosome (Chiang et al., 1989; Dice, 1990). The delivery relies on binding of Hsc70 to the lysosome-associated membrane protein type 2A (LAMP-2A), a CMA receptor at the lysosomal membrane (Cuervo and Dice, 1996). Then, the substrate protein is unfolded and subsequently translocated into the lysosomal lumen across the membrane for degradation. Microautophagy, the least studied autophagic pathway, is mediated by direct lysosomal engulfment (Li et al., 2012). Despite the different mechanisms, all three types of autophagy help maintain the cellular homeostasis and turn cellular components to energy. This thesis would mainly discuss macroautophagy, hereafter refers to as autophagy.

1.2.1 Regulation of the autophagic pathway

Autophagy is a highly dynamic process happening all the time in cells. Under starvation, autophagy is dramatically induced, which is achieved through phagophore generation, phagophore engulfment of cargos, autophagosome maturation, and autophagosome-lysosome fusion. After the fusion between the outer membrane of the autophagosome and lysosome, the inner membrane of the autophagosome quickly gets degraded followed by exposure and degradation of the cargo (Rabinowitz and White, 2010).

The formation of the phagophore and autophagosome is a hierarchically orchestrated process, which requires the involvement of a series of autophagy proteins (ATGs). ATGs were first identified in yeast through a genetic screen for autophagy-regulating proteins and later were found to be highly conserved in higher eukaryotes including humans (Klionsky et al., 2003). In addition to the requirement of ATGs, autophagy is distinguished from proteasome-dependent degradation through its need for a source of the membrane to generate autophagosomes. Recent studies show the membrane source can be various, such as ER, mitochondria, nuclear envelope and ER-Golgi intermediate compartment (ERGIC) (Axe et al., 2008; Ge et al., 2013; Hayashi-Nishino et al., 2010; Kawabata and Yoshimori, 2016). A triple coloured live-cell imaging study even showed isolation membrane formation at contact sites between ER and mitochondria (Hamasaki et al., 2013). Among all the membrane sources, ER-derived isolation membrane generation is the most studied autophagosome formation in mammalian cells (Figure 1.1).

ULK1 plays a central role in the initiation of autophagy. In nutrient rich conditions, sensing of high amino acid levels in lysosomes by the v-ATPase activates Rag GTPase. Activated Rag GTPase binds to the mechanistic target of rapamycin complex 1 (mTORC1) and leads to phosphorylation and inactivation of ULK1 (Hosokawa et al., 2009; Sancak et al., 2008; Zoncu et al., 2011). Under starvation, the amino-acid level in the lysosome drops, resulting in the dissociation of mTORC1 from lysosomes which leads to dephosphorylation and activation of ULK1 and ATG13 (Hosokawa et al., 2009; Kim et al., 2011; Sancak et al., 2008; Zoncu et al., 2011). The activated ULK1 complex, composed of ULK1, ATG13, ATG101 and FIP200, translocates to the ER surface, where it facilitates recruitment of other factors in a hierarchical fashion (Kawabata and Yoshimori, 2016). Class III PI3K complex, consisting of Beclin1, VPS34, ATG14 and VPS15, is first recruited to the ER surface after the translocation of the ULK1 complex

(Karanasios et al., 2013). Activated class III PI3K complex synthesizes PtdIns3P (PI3P), which induces nucleation of the so-called omegasome on the surface of the ER. The existence of PI3P provides a positive loop that promotes the recruitment of additional components of the ULK complex and stimulates the elongation of the omegasome (Burman and Ktistakis, 2010). PI3P also aids the recruitment of WIPIs, the mammalian orthologue of yeast Atg18, to the isolation membrane which has been shown to be required for the recruitment the ATG12 complex (see below) (Dooley et al., 2014). ATG9, the only transmembrane protein involved in autophagosome formation, is another key regulator of autophagy induction and is thought to provide the membrane or to retrieve intermediate components during autophagosome formation (Reggiori and Tooze, 2012).

The ubiquitin-like conjugation systems are then recruited to the isolation membrane, which lipidates ATG8 proteins and expands the isolation membrane. In yeast, there is only one Atg8 protein, while there are six known ATG8 proteins in mammalian cells. These include three members of the microtubule-associated protein 1 light chain 3 (MAP1LC3) subfamily (LC3A, LC3B and LC3C) and three members of the gamma-aminobutyric receptor-associated protein (GABARAP) subfamily (GABARAP, GABARAP-L1 and GABARAP-L2/GATE-16) (Shpilka et al., 2011). Processed by two ubiquitin-like conjugation systems, LC3 becomes membrane-associated and recruited from the cytoplasm to the autophagosome surface (Ichimura et al., 2000; Mizushima et al., 1998). First, LC3 is processed at its C-terminus by the ATG4B protease. The cleaved LC3 is then activated by ATG7 (E1 activating enzyme), followed by conjugation with ATG3 (E2 activating enzyme) and modification with phosphatidylethanolamine (PE) by the ATG12 complex (E3 activating enzyme). Since the lipidated form of LC3 migrates faster on an SDS-polyacrylamide gel and is distinguishable from cytosolic LC3, LC3-PE is usually referred as

LC3-II and is used as a marker for autophagic flux (Klionsky et al., 2016). As the isolation membrane expands, the ULK1 complex disassociates from the ER with the omegasome ring starting to enclose. When the enclosure is complete, the omegasome collapses back to the ER (Axe et al., 2008), and the isolation membrane seals as an autophagosome, which releases from the ER to fuse with a lysosome (Karanasios et al., 2013). Before fusion, the LC3-II on the outer membrane is cleaved by ATG4B.

The regulation of fusion between the autophagosome and lysosome is not well understood. Studies show that the SNARE protein syntaxin 17 (STX17) on the surface of completed autophagosomes tethers the autophagosome and lysosome (Itakura et al., 2012; Jiang et al., 2014). STX17 is recruited to autophagosomes at the late stage of autophagosome formation and shows a strong degree of co-localization with LC3. During the fusion event, STX17 interacts with SNAP-29 and VAMP-8, which mediates the fusion between the lysosome and the outer membrane of the autophagosome. Soon after fusion, the inner membrane is degraded followed by the exposure and degradation of contents as well as a portion of LC3-II (Mizushima and Komatsu, 2011). The degradation is followed by the recycling of breakdown components to be used in bioenergetic and the anabolic pathways.

When induced by starvation, the autophagic machinery nucleates an isolation membrane independent of any bound cargo. However, along with LC3 recruitment to the isolation membrane, cargo-bound cargo receptors are also recruited. Cargo receptors selectively tether their cargo to the isolation membrane, but the random cytoplasmic material is also engulfed by the forming isolation membrane. Because the matured autophagosomes contain both selective cargos and random material, the starvation-induced autophagy is considered as non-selective autophagy.
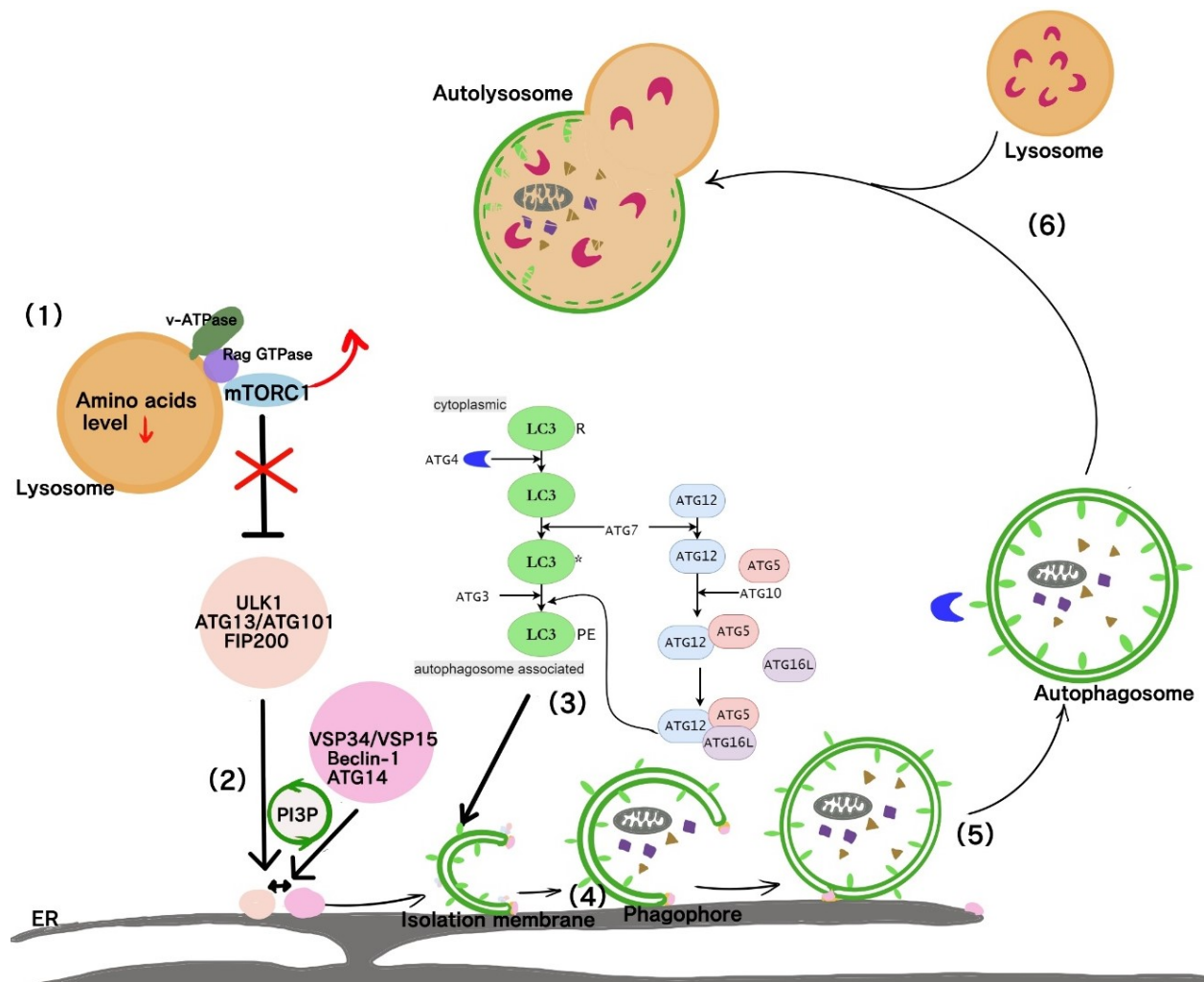
Figure 1.1 The regulation of autophagy.

(1) Low amino acids level in the lysosome results in the inactivation of mTORC1 and the activation of ULK1. (2) The recruitment and activation of PI3K by ULK1 complex leads to the generation of PI3P. (3) Processing of LC3 and its attachment to the isolation membrane promote the expansion of isolation membrane. (4) As expanded, the isolation membrane becomes phagophore and engulfs the cytosolic materials for degradation. (5) Phagophore seals to autophagosome and buds from ER membrane, with the LC3-II on the outer membrane cleaved by ATG4B. (6) The engulfed material is then transported to the lysosome by fusion with the autophagosome.

1.2.2 Selective autophagy

Different from the starvation condition, in which autophagosome formation is thought to be triggered independently of any cargo, in non-starved cells, autophagosome generation depends on cargo recognition (Zaffagnini and Martens, 2016). In non-starved condition, cells undergo basal autophagy with selectivity to maintain cellular homeostasis. Selective autophagic pathways are usually named after the cargo to be degraded, such as ER-phagy (ER), mitophagy (mitochondria), aggrephagy (protein aggregates), ribophagy (ribosomes), lipophagy (lipid droplets), ferritinophagy (ferritin), and xenophagy (pathogens, including bacteria) (Khaminetsm et al., 2016; Kraft et al., 2008; Mancias et al., 2014; Singh et al., 2009). The specificity depends on selective receptor proteins, which physically bind their cargo to a nascent autophagosome through interaction with ATG8-family proteins (Rogov et al., 2014). Based on the different mechanisms of cargo recognition, the selective autophagy receptors can be categorized into two groups: ubiquitin-dependent and ubiquitin-independent. The known ubiquitin-dependent receptors include p62/SQSTM1, NBR1, OPTN, TAXIBP1, NDP52/CALCDCO2, TOLLIP, and RPN10 (Mancias and Kimmelman, 2016). They bind ATG8-PE proteins via their LC3-interacting regions (LIR), and they also have the ability to bind ubiquitin chains through ubiquitin binding domains (UBD) (Kraft et al., 2010). Different from ubiquitin-mediated cargo binding, ubiquitin-independent selective autophagy receptors activate selective autophagy through directly binding to intracellular cargo by recognition of specific types of signals on proteins, lipids, or sugars.

How does ubiquitin-dependent selective autophagy work? First, autophagic substrates are tagged by ubiquitin chains with a high local concentration (Figure 1.2). Then, the ubiquitin-dependent selective autophagy receptors are recruited to the cargo site via high-affinity or high-avidity interactions with the ubiquitin chains. Notably, receptors show preferential binding to

certain types of ubiquitin chains. K63-linked ubiquitin chains are preferred by p62/SQSTM1 binding, while K48-linked chains are recognized by proteasomes (Seibenhener et al., 2004). Additionally, selective autophagy receptors show preferential binding to multiple ubiquitin chains, suggesting the division of work for autophagic and proteasomal degradation (Zaffagnini and Martens, 2016). Through interactions with cargo receptors, autophagic machinery is hierarchically recruited to the cargo site after receptor binding. Once recruited to the cargo, the autophagic machinery is activated and drives the nucleation of an isolation membrane close to the cargo. The isolation membrane further elongates to form a complete autophagosome surrounding the cargo. High-avidity interactions between cargo receptors and membrane-associated ATG8-family proteins ensure the exclusion of other cytoplasmic material and achieve the selectivity.

Autophagy is essential for cellular quality control, cell survival in a stressed situation as well as differentiation and development events. Therefore, failures in autophagy are broadly associated with diseases such as neurodegeneration, metabolic diseases, and cancer (Jiang and Mizushima, 2013).
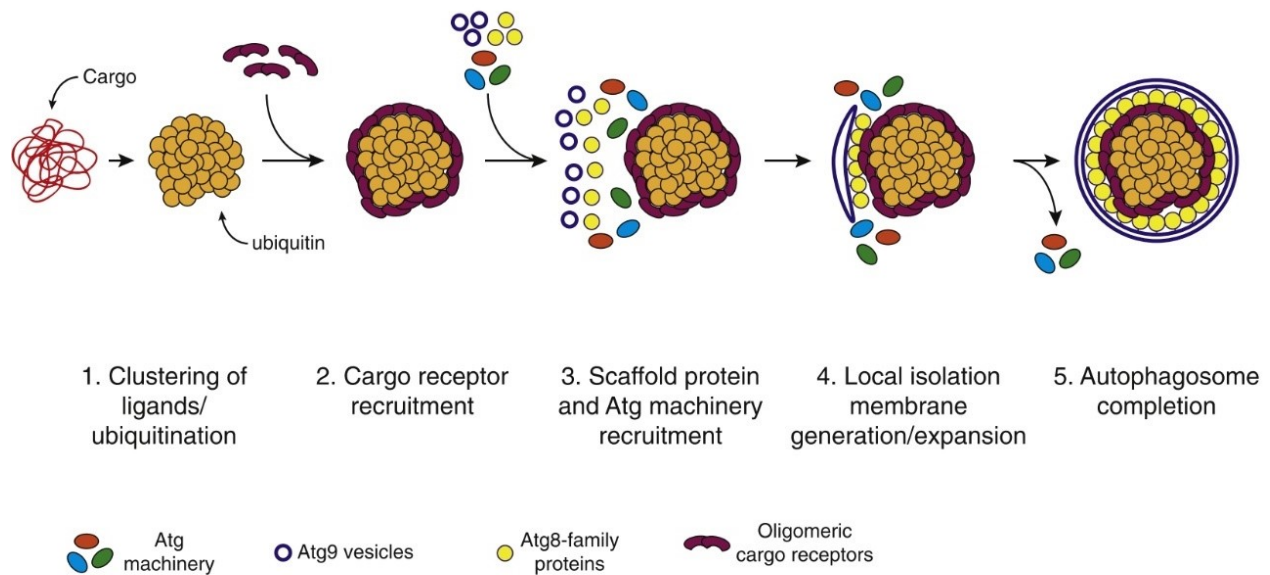
Figure 1.2 The generation of selective autophagosome. (Adapted from Zaffagnini and Martens, 2016) See text for details.

1.2.3 The roles of trafficking proteins in autophagy

One main characteristic of autophagy is the double-membrane autophagosomes, whose formation requires an adequate supply of membranes and appropriate cellular membrane dynamics. In yeast *Saccharomyces cerevisiae*, autophagosomes are generated at distinct cellular locations called phagophore assembly sites (PAS) (Suzuki et al., 2001). Atg9 vesicles have been shown to move dynamically between PAS and peripheral sites after autophagy induction (Sekito et al., 2009). As the only known transmembrane Atg protein, Atg9 is essential for autophagosome formation, since nonfunctional Atg9 causes decreased autophagy activity (Feng et al., 2016). Studies indicate the Atg9 cycling contributes to autophagosome formation by supplying membranes to the autophagosome (Reggiori et al., 2005; Yen et al., 2007). Although a specific site for

autophagosome formation like PAS is absent in mammalian cells, ATG9 also redistributes in an Ulk1-dependent manner in response to autophagy induction. ATG9 displays dynamic cycling between the trans-Golgi network and endosomes in nutrient-rich conditions, and becomes more dispersed and transiently colocalizes with LC3-positive structures during starvation (Young et al., 2006). Growing evidence supports the theory that ATG9 is required for transport between endocytic and autophagic compartments. However, whether this transportation is a delivery of factors to the isolation membrane or a retriever of factors from the isolation membrane remains controversial.

RAB GTPases, RAB GTPase-Activating Proteins (GAPs) and RAB GEFs have been shown to be involved in ATG9 trafficking. Studies in *Saccharomyces cerevisiae* indicate that the small Rab GTPase Ypt1 and its GEF, the TRAPP III complex, play important roles in autophagosome formation (Lynch-Day et al., 2010). The TRAPP III unique subunit Trs85 recruits TRAPP III to the PAS via its adaptor protein Trs20, where the complex actives Ypt1 to regulate the assembly of the PAS (Lipatova et al., 2012; Lynch-Day et al., 2010; Taussig et al., 2014). Ypt1 and Atg9 are found colocalized on the PAS and also in cytosolic puncta (Lipatova et al., 2012). However, whether Atg9 recruits TRAPP III or vice versa is still unclear. Similarly, TRAPP III has also been shown to regulate ATG9 trafficking and autophagy in human cells through interaction with TBC1D14, a TBC domain-containing RAB GTPases activating protein (RAB GAP) (Lamb et al., 2016). In addition to TBC1D14, other RAB GAPs such as TBC1D5 also mediate ATG9 trafficking (Popovic et al., 2014).

Autophagosome-lysosome fusion is another process requiring the function of membrane trafficking regulators. Besides the previously discussed SNARE protein STX17, RAB7 has been shown to be the main regulator. This regulatory function, which is found both under nutrient rich

and starvation conditions, relies on its binding and hydrolysis of GTP. Activation of Rab7 through the homotypic fusion and protein sorting complex (HOPS) and UV radiation resistance-associated gene (UVRAG) stimulates autophagosome maturation and fusion with lysosomes (Gutierrez et al., 2004). Yeast Ypt7 (Rab7 orthologue) mutants display cytoplasmic accumulation of autophagosomes (Kirisako et al., 1999).

1.3 Lipophagy

Autophagy is also involved in the degradation of cellular lipid stores. In cells, fatty acids are stored as triglycerides in highly dynamic organelles called lipid droplets (LDs) (Beller et al., 2010). LDs are surrounded by a phospholipid monolayer and LD coat proteins called perilipins (PLINs). When necessary, fatty acids can be released from LDs through a cytosolic lipase- (ATGL) mediated process named lipolysis or through an autophagic digestion process called lipophagy. The lipophagy process was first described in cultured hepatocytes, as co-localization between LDs and lysosomes was observed and disruption of autophagy increased both the size and number of cellular LDs (Singh et al., 2009). In addition, PLINs were found in the autophagosomes and lysosomes isolated from starved cells, and purified LDs also showed association with LC3-II. Later, the involvement of autophagy in lipid storage regulation was broadly shown in most cell types as well as in different organisms such as *Saccharomyces cerevisiae* (van Zutphen et al., 2014), *Caenorhabditis elegans* (Lapierre et al., 2011) and rice (Kurusu et al., 2014).

In this process, similar to macroautophagy, portions or whole LDs become trapped inside the double-membrane-bound autophagosome vesicles and are transported to lysosomes to get degraded. Notably, the conversion of LC3-I to LC3-II happens on the surface of LDs, similar to

what was described above for the assembly of autophagy machinery. Moreover, CMA is also shown to have a significant role in LD turnover (Kaushik and Cuervo, 2015). CMA degrades PLIN2 and PLIN3 on LD membranes and facilitates the access of the cytosolic lipase to the lipid core. Concurrently, elimination of PLINs allows autophagosome formation-associated proteins to access the LD core, which also facilitates liphophagy (Figure 1.3).

The suppression of lipophagy is associated with fatty liver disease, characterized by abnormal accumulation of lipids in the liver. Mice fed with a high-fat diet show a suppressed lipophagy, as a decreased level of LD-associated LC3 is found (Singh et al., 2009). Liver-specific ATG7 knockout mice with defective autophagy show larger livers with elevated lipid content, while in contrast, liver-specific overexpression of ATG7 ameliorates high fat-induced hepatic inflammation, ER stress and hepatic steatosis (Singh et al., 2009; Yang et al., 2010). Moreover, obesity is corelated with hyperactivation of mTORC1 signaling which strongly inhibits autophagy. On the other hand, it has been shown that a prolonged high-fat diet blocks the fusion of autophagosomes and lysosomes (Koga et al., 2010) as well as inhibits CMA (Rodriguez-Navarro et al., 2012). Given the role for CMA in the degradation of PLINs, it is conceivable that blockage of CMA would hinder lipophagy and eventually promote lipid accumulation.

As mentioned above, TRAPPC11 is implicated in lipid mobilization in liver. Considering the fatty liver phenotype of *fgr* zebrafish (Sadler et al., 2005), the liver steatosis in a *TRAPPC11* patient (Liang et al., 2015) and the abundant lipid droplets in *TRAPPC11* mutant fibroblasts (DeRossi et al., 2016), it is tempting to speculate on a role of TrappC11 in autophagy, especially in lipophagy.
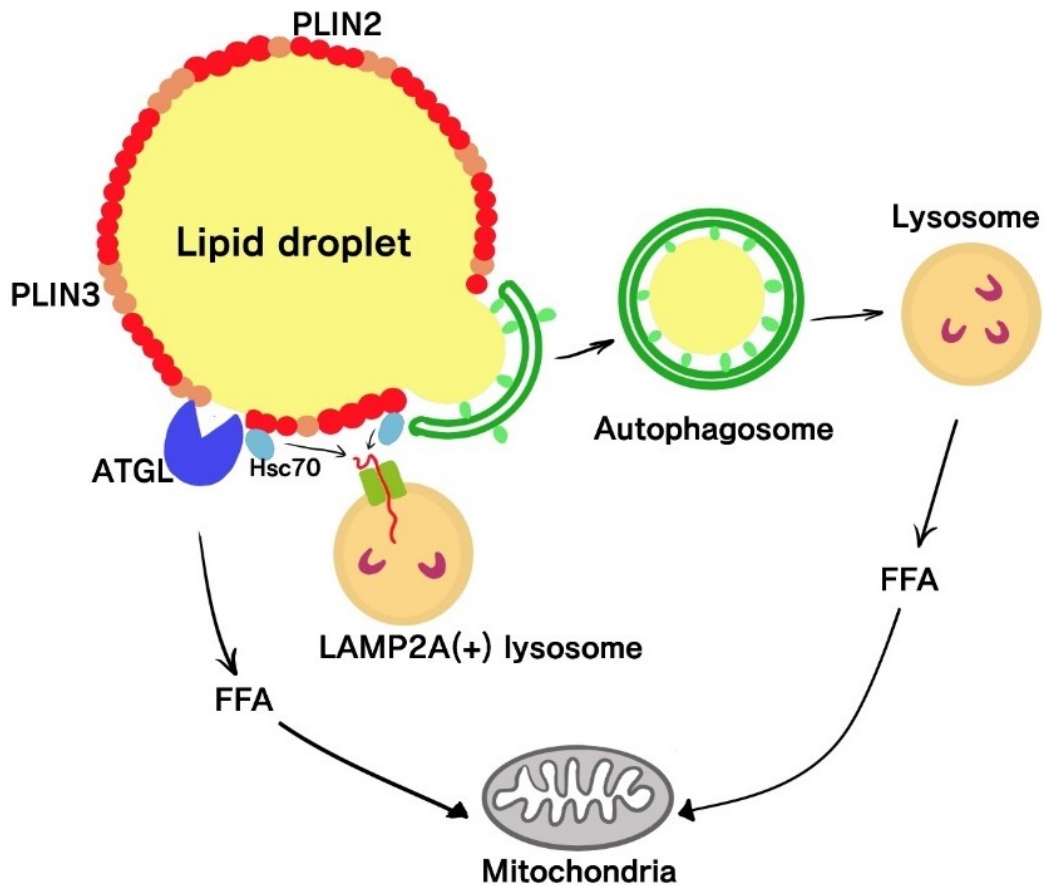
Figure 1.3 CMA facilities LD turnover through lipophagy and lipolysis.

Hsc70 recognizes PLINs and brings a single PLIN protein to LAMP2A-positive lysosomes for degradation via CMA. The depletion of PLINs exposes the LD core to lipase (ATGL) and autophagy machinery, which facilitates lipolysis and lipophagy, respectively. Through cytosolic lipase or lysosomes, the LD turns to free fatty acids and provides energy for cellular processes.

Chapter 2: Materials and Methods

2.1 Plasmid Construction

To obtain BirA*-FLAG-tagged TRAPPC11 plasmids for generating BioID cell lines and eGFP-TrappC11 plasmids for fluorescent microscopy for TrappC11, molecular cloning techniques using Gateway® were applied. The plasmids and primers used for cloning are listed in Tables 2.1 and 2.2, respectively.

2.1.1 BP recombination

The BP recombination was employed to obtain a TRAPPC11 entry clone plasmid. Recombination mixture was set up with 1 µL 50 ng/µL pDONR 201 plasmid, 1 µL purified PCR product of TRAPPC11, 1 µL TE buffer (10 mM Tris-HCl pH 8.0, 1 mM EDTA) and 0.5 µL BP recombination enzyme (Invitrogen). A negative control was also set up with the same components but without recombination enzyme. The mixtures were incubated at 25°C overnight followed by bacterial transformation. Entry clone plasmids were purified using a plasmid miniprep kit (Bio Basic) and further confirmed by *Bsr*GI (NEB) digestion.

2.1.2 LR recombination

The LR recombination mixture was set up with 1 µL destination plasmid (50 ng/µL), 1 µL TRAPPC11 entry clone plasmid prepared from a miniprep (50 ng/µL), 1 µL TE buffer and 0.5 µL LR recombination enzyme (Invitrogen). A negative control was also set up with the same components but without recombination enzyme. Mixtures were incubated at 25°C overnight

followed by bacterial transformation. Destination plasmids were purified using a plasmid miniprep kit (Bio Basic) and further confirmed using *Bsr*GI digestion.

2.1.3 Bacterial Transformation

For bacterial transformation, 75 µL DH5α competent cells (Invitrogen) were mixed with the recombination reaction or control and kept on ice for 30 minutes. Cells were heat shocked in a 42°C bath for 90 seconds and immediately cooled down on ice for 3 minutes. The cell mixture was then added into 1 mL LB medium (1% Tryptone, 1% NaCl, 0.5% Yeast extract) and incubated at 37°C with shaking for 1 hour. Cells were spread on LB plates containing 20 µg/ml kanamycin (BP cloning) or 50 µg/ml ampicillin (LR cloning) and incubated at 37°C overnight. Colonies on the ligation plate were inoculated into 2 mL LB medium and cultured overnight for plasmid extraction and verification.

Table 2.1: Plasmids used in this study

Plasmids	Bacterial selection	Source
pENTR201-TRAPPC11	Kanamycin	Open Biosystems
pDONR201	Kanamycin	Sacher Lab
pDEST_pcDNA5_BirA*-FLAG_Nterm	Ampicillin	Gingras lab
pDEST_pcDNA5_BirA*-FLAG_Cterm	Ampicillin	Gingras lab
pOG44	Ampicillin	Gingras lab
pcDNA-eGFP-GWY1	Ampicillin	Sacher Lab
Alt-R™ S.p. Cas9 plasmid	Ampicillin	IDT

Table 2.2: Primers used in this study

Primers	Sequence
C11-F-GWY-kozak	GGGGACAAGTTTGTACAAAAAAGCAGGCTTCACCATGAGCCCCACAC AGTGGGACTTC
C11-R-GWY-no stop	GGGGACCACTTTGTACAAGAAAGCTGGGTGTGCAGCAGCAATAGAG GTATCATC
C11_CRISPR-newF2	GTTGGGATTGTATGCGTGAG
C11_CRISPR-newR1	TCACAATGCCATTACCTTGG
gryseq1F	GGAGAAGATGTCATTGCTTCAG
gryseq2F	CCTGGTTTCTATTACCAGCAGGC
gryseq3F	AAGTCCTGATCCAGAACCCGAC
gryseq4F	CTTACAGGCAGCTCGGTCTTTC
gryseq5F	GATGACGGACCTCTTAAGTGC

2.2 Electrophoresis, Western Blotting

2.2.1 Electrophoresis

For analysis of DNA fragments, PCR products or digested plasmids were loaded on a 1% agarose gel with RedSafe (FroggaBio, 1:20000). The electrophoresis was performed at 100 volts for 30 minutes and the gels were examined using Syngene G:BOX EF3 imager.

2.2.2 Western blot

For analysis of proteins in cell lysates, samples of 20 µg proteins were fractionated on 8% or 15% SDS-polyacrylamide gels. The proteins were transferred to nitrocellulose membranes for 1 hour at 100 volts or overnight at 30 volts. Membranes were blocked with 5% skim milk powder

in PBS-T (PBS with 0.1% Tween 20). The primary and secondary antibodies were incubated in

PBS-T for 1 hour each. Antibodies used and their dilutions are listed in Table 2.3. Signals were

detected using ECL reagent (GE Healthcare) and exposed on an Amersham Imager 600 (GE

Healthcare).

Table 2.3: List of antibodies used in this study

Antigen	Type	Host	IF dilution	WB dilution	Size (kD)	Catalog number	Source
FLAG	M	m	N/A	1:5,000	N/A	F1804	Sigma
Tubulin	M	m	N/A	1:5,000	50	T6199	Sigma
P115	M	m	1:250	N/A	N/A	N/A	Shields lab
GM130	P	r	1:250	N/A	N/A	N/A	Lowe lab
ManII	P	r	1:250	N/A	N/A	N/A	Moremen lab
p62/SQSTM1	P	r	1:500	N/A	N/A	ab207306	Abcam
LC3B	P	r	1:250	1:1000	13	ab192890	Abcam
LAMP1	P	r	1:300	N/A	N/A	ab24170	Abcam
TrappC11	P	r	N/A	1:500	129	N/A	Sacher lab
TrappC12	P	r	N/A	1:2,500	78	N/A	Sacher lab
Secondary IgGs							
Alexa Fluor 568 anti–mouse	HCA	g	1:500	N/A	N/A	A-11031	Life Tech.
Alexa Fluor 647 anti–rabbit	HCA	g	1:500	N/A	N/A	A-21245	Life Tech.
HRP-labeled anti–mouse	P	g	N/A	1:5,000	N/A	KP-474-1806	KPL
HRP-labeled anti–rabbit	P	g	N/A	1:5,000	N/A	KP-474-1506	KPL

All protein sizes are in kilodaltons. N/A, not applicable; M, monoclonal; P, polyclonal; HCA, highly cross-adsorbed; r, rabbit; m, mouse; g, goat; h, human; IF, immunofluorescence; WB, Western blotting.

2.3 Immunofluorescent microscopy

In order to observe cellular components, cells were grown on coverslips and fixed with 4% PFA for 20 minutes after washing with PBS. Following fixation, cells were permeabilized with 0.1M glycine in PBS for 10 minutes and 0.1% Triton X-100 in PBS for 10 minutes. After permeabilization, cells were blocked with PBS containing 5% normal Goat serum for 45 minutes at room temperature. Primary antibodies (Table 2.3) and BODIPY 490/503 (Life Technologies, 1:1000) were diluted in PBS containing 5% normal Goat serum and incubated overnight at 4°C in 50 µL volumes on coverslips. Before secondary antibody incubation, coverslips were washed twice with PBS. Secondary antibodies (Table 2.3) and DAPI (1:1000) were diluted as above and incubated in the dark for 1 hour at room temperature. Washes after secondary antibodies incubation were as above. Coverslips were mounted on slides using Antifade Gold (Invitrogen) mounting medium and observed using a Nikon C2 laser scanning confocal microscope fitted with a Plan Apo Lambda 100× oil objective (Nikon). Capture of images with 1024×1024 pixel resolution was controlled by NIS Elements C 4.4 software. Z stacks were acquired with a 0.2 µm increment. Identical intensity and exposure settings were used for control and experimental conditions.

2.4 Cell culture

The cell lines used in this study are listed in Table 2.4. For general culture, cells were cultured in complete medium (90% DMEM with high glucose and L-glutamine + 10% FBS) at 37ºC in cell culture incubators (5% CO_2 with humidity). For starvation, cells were washed 3 times with PBS, then incubated with EBSS medium.

Table 2.4: Cell lines used in this study

Cell line	Culture medium	Source
Flp-In/T-REx 293	DMEM (high glucose, L-glutamine) with 10%FBS, 100 µg/ml Zeocin (Invitrogen), and 15 µg/ml Blasticidin (Bioshop)	Life Tech.
HeLa	DMEM (high glucose, L-glutamine) with 10%FBS	Sacher lab
HeLa LC3-GFP-RFP	DMEM (high glucose, L-glutamine) with 10%FBS	Sacher lab

2.4.1 Cell freezing and thawing

Cells to be frozen were trypsinized, collected and pelleted in sterile tubes (1,700 RPM, 3.5 minutes). The cell pellets were gently resuspended with freezing medium (70% DMEM with high glucose and L-glutamine + 20% FBS + 10% DMSO), transferred into freezing tubes and stored at -80°C or in liquid nitrogen.

To thaw frozen cells for starting a new culture, the tubes containing frozen cells were incubated in a 37°C bath until the cells were completely thawed. The cells with freezing medium were transferred into a 10-cm dish containing 10 mL fresh complete medium and incubated in a 37°C incubator overnight. The next day, the medium was changed with fresh complete medium to remove the maintaining freezing medium. Notably, when thawing the Flp-In/T-REx 293 cell line, the medium did not contain any antibiotic within the first 24-hour culture.

2.4.2 RNA interference

To study the effect of TrappC11 knockdown, HeLa cells were transfected twice with 60 nM siRNA against TrappC11 (5'- GGAUUUAUAAACUACAAGGATT- 3') (Life Technologies) using JetPrime (Polyplus) as described in the manufacturer's protocol. One day before the first

transfection, cells were trypsinized and replated at a density of 50% confluency. Cells were split one day after transfection and treated with the second transfection 48 hours after the first transfection. 48 hours after the second transfection, cells were trypsinized and replated for experiments. Cells were analyzed by western blot analysis or by fluorescent microscopy 3 days after the second siRNA treatment.

2.5 BioID

To identify the interacting proteins of TrappC11, two inducible cell lines expressing BirA*-tagged TrappC11 were generated and used for BioID purification followed by mass spectrometry analysis.

2.5.1 Generating BioID cell line

The Flp-In/T-REx 293 cell line from Life Technologies (R780-07) was used to generate BioID cell lines. Parental cells were seeded in a 10 cm dish with medium containing complete medium with 15 ug/ml Blasticidin one day before transfection to obtain 70% confluency on the day of transfection. The transfections were performed using Jetprime (Polyplus). For each 10 cm dish, a mixture of 500 µL buffer, 1.5 µg BirA*-FLAG construct, 13.5 µg pOG44, and 30 µl Jetprime transfection reagent was prepared. After 10-minute incubation, the mixture was added to the dish and the medium was gently mixed. The dishes were then incubated in a 37°C incubator for 24 hours before changing the medium with fresh antibiotic-free complete medium.

48 hours after transfection, cells were split at 1:4 dilutions (or 25% confluence) to two 10 cm dishes. 100 µg/ml hygromycin and 15 µg/ml blasticidin were added to start the antibiotic

selection. The medium was changed every 2-3 days during the 2-week selection until colonies were visible and ready to be picked up. Colonies were picked up by a pipet tip to obtain monoclonal cell lines or mixed to get a polyclonal cell line. Cell lines were maintained in complete medium with 100 µg/ml hygromycin and 15 µg/ml blasticidin.

Two control cell lines were generated by transfecting Flp-In/T-REx 293 cells with pDEST_pcDNA5_BirA*-FLAG_Nterm or pDEST_pcDNA5_BirA*-FLAG_Cterm plasmid followed by selection as described above.

2.5.2 Testing the expression of BioID cell lines

The capability of expressing BirA*-FLAG-fusion protein of the cell lines was tested after obtaining the cell lines. Cells were plated in 6-well dishes, and a final concentration of 1 µg/ml tetracycline was added to induce expression. 24 hours after induction, cells were collected. Expression of the fusion protein was examined using a FLAG antibody through western blotting analysis.

2.5.3 BioID Purification

To obtain purified TrappC11-interacting proteins, BirA*-fusion TrappC11 cells and BirA* control cells were grown in 15 cm dishes with 15 mL complete medium. When cells reached 60% confluency, they were treated with 50 ng/mL tetracycline. 16 hours after induction, the medium was changed with 15 mL pre-warmed DMEM (high glucose, L-glutamine) supplemented with 20% FBS, 50 ng/mL Tetracycline in combination with 50 µM biotin. After 8 more hours, cells were pelleted and lysed in ice-cold RIPA buffer (50 mM Tris pH 7.4, 150 mM NaCl, 1% NP-40, 0.5%

Sodium Deoxycholate, 0.1% SDS, 1 mM EDTA) supplemented with complete-mini protease inhibitor cocktail (Roche), 1 mM PMSF, 62.5 Units/mL Benzonase (Invitrogen), and incubated at 4°C for 1 hour. Samples were sonicated in 4°C ice bath, with 4 times of 10-second low power bursts. After sonication, samples were centrifuged at 4°C for 30 minutes at 13,200 RPM in a refrigerated microfuge. Supernatants were incubated with 14μL streptavidin-Sepharose beads (Sigma) at 4°C for 3 hours to capture the denatured biotinylated proteins. After the incubation, beads were washed five times with RIPA and four times with low-detergent buffer (25 mM Tris pH7.4, 100 mM NaCl, 0.025% SDS). Following the last wash, beads were pelleted and stored at -80°C. Beads with purified biotinylated proteins were sent for mass spectrometry or analyzed by western blot.

2.5.4 Mass spectrometry

Mass spectrometry was used to identify proteins captured by the BioID purification. Mass spectrometry was performed by Dr. Tommy Nilsson's laboratory. Data were analyzed in Scaffold 4 proteomic software. Proteins with 95% confidence and more than two unique peptides identified in induced cell lines and negative results in control were considered as interacting proteins.

2.6 CRISPR

To generate TrappC11 knockout cell lines, the CRISPR method was used. By introducing Cas9 enzyme and crRNA:tracrRNA complex into cells, a double-strand break would be generated in the chosen region of genomic DNA. Through DNA repairing *via* non-homologous end joining,

frameshift mutations which possibly lead to nonfunctional protein could be introduced into the cells.

2.6.1 Transfection with the Cas9 expression plasmid

HeLa cells were trypsinized and plated in a 10 cm dish to obtain 70–80% confluency on the day of transfection. The transfection solution was prepared with 1000 µL transfection buffer, 15 µg Alt-R^{TM} *S.p.* Cas9 plasmid (IDT), 30 µL Jetprime transfection reagent (Polyplus), and incubated at room temperature for 15 minutes to form transfection complexes. Medium without antibiotics was replaced for the plated cells, and transfection complex was added after the 15-minute incubation. Six hours after transfection, the medium was replaced with 20 mL of fresh complete medium, and the plate was incubated in a tissue culture incubator for 24 hours.

2.6.2 Delivery of Alt-RTM CRISPR RNAs

TrappC11 crRNA (IDT) and common tracrRNA (IDT) were resuspended in Nuclease-Free Duplex Buffer (IDT) to 100 µM final concentrations. 0.75 µL of crRNA (100 µM), 0.75 µL tracrRNA (100 µM), and 23.5 µL Nuclease-Free Duplex Buffer were mixed in a sterile RNase-free PCR tube. The mixture was heated at 95°C for 5 minutes and removed from heat to cool to room temperature (15–25°C).

A mixture with 50 µL transfection buffer, 7.5 µL crRNA:tracrRNA complex and 2 µL Jetprime transfection reagent (Polyplus) was incubated at room temperature for 15 minutes to form transfection complexes. During incubation, cells transfected with Cas9 plasmid were trypsinized and diluted using complete media to obtain 75% confluency. The transfection complexes were

added to a well of a 24-well dish with 500 µL of diluted cells (final concentration of Alt-R^{TM} CRISPR RNAs was 30 nM) and incubated in a tissue culture incubator (37°C, 5% CO_2) for 48 hours.

2.6.3 Isolation of monoclonal cell lines

After 48-hour incubation, CRISPR RNA-transfected cells were trypsinized and collected in a centrifuge tube. Cell number was counted and 10 cm plates with 50, 250, 1000, and 5000 cells were prepared. Two weeks after plating, cell colonies were picked up and grown in 6-well dishes. Monoclonal cell lines were tested and frozen after reaching 90% confluency.

2.6.4 Verify the knockout cell clones

The mutants of TRAPPC11 were tested by T7E1 assay and western blotting.

2.6.4.1 T7E1 assay screening

Genomic DNAs of monoclonal cell lines were isolated for T7E1 assay. Cell pellets were resuspended in 350 µl Tris-EDTA buffer (50 mM Tris-HCl pH7.5, 20 mM EDTA), mixed with 40 µl 10% SDS, and heated at 65°C for 30 minutes. 100 µl of 5 M KOAc were added, followed by a 10 minute incubation on ice. Supernatants obtained from a 5 minute centrifugation at 13,000 rpm were transferred into a new tube and mixed with 2 volumes of 99% ethanol. Precipitated DNAs were obtained with a 5 minute centrifugation at 13,000 rpm and washed with 70% ethanol. The lids of the tubes were opened for 10 minutes to allow the remaining ethanol to evaporate. The genomic DNA pellets were dissolved in 100-200 µL TE buffer and used as templates for a PCR reaction as below:

10x Standard Taq Buffer	5 μL
C11_CRISPR-newF2 (5 μM)	5 μL
C11_CRISPR-newR1 (5 μM)	5 μL
dNTP (2 μM)	5 μL
Taq	1 μL
Genomic DNA	1 μL
H2O	28 μL
Total Volume	50 μL

PCR products were then fractionated on a 1% agarose gel and the target bands were cut and extracted from the gel. 1 μL 10x NEB Buffer 2.1 was mixed with 9 μL cleaned PCR products in a clean PCR tube and the annealing program was performed in a thermal cycler as below:

95ºC for 5 minutes, decrease the temperature from 95ºC to 85ºC with 2ºC decrease per second and decrease the temperature from 85ºC to 25ºC with 0.1ºC decrease per second.

Following annealing, 0.25 μL T7E1 (NEB) was added to each tube and digested for 20 minutes at 37ºC. The digestion mixture was examined by electrophoresis on a 2% agarose gel for 40 minutes at 100 volts.

2.6.4.2 Immunoblot analysis

The cell lines were collected and lysed with lysis buffer (50 mM Tris pH7.2, 1 mM EDTA, 150 mM NaCl, 1 μM DTT, 1% Triton-X100) supplemented with complete-mini protease inhibitor cocktail (Roche). The expression levels of TrappC11 for the cell lines were then examined by western blotting.

Chapter 3: Results

3.1 Generation of inducible TrappC11 BirA*-fusion cell lines

To identify the proteins that interact with TrappC11, I employed the BioID technique (Roux et al., 2012). In this method, BirA*-fused TrappC11 is introduced into cells by transfection. Upon addition of biotin, BirA*, as a biotin ligase, catalyzes the biotinylation of proteins within close proximity to TrappC11 (Figure 3.1 A). After collecting cell lysates and capturing biotinylated proteins with streptavidin agarose, interacting proteins were identified by mass spectrometry.

To avoid unspecific biotinylation caused by overexpression of BirA*-TrappC11, an inducible cell line expressing TrappC11 with the BirA*-FLAG tag was generated. To identify the interactions without the effect of the tags to the normal function of TrappC11, two plasmids with different orientations of BirA*-FLAG tag were constructed and used for generating the cell lines (Figure 3.1 B). The expression of the tag fused to TrappC11 in these two cell lines was tested. These inducible cell lines can only express BirA*-FLAG-tagged TrappC11 after tetracycline induction (Figure 3.1 C).

To reduce the side effect of overexpression of TrappC11 on normal cell function, I tested the fusion protein expression under different tetracycline concentrations (Figure 3.2 A). The data demonstrated that 50 ng/mL tetracycline leads to a reasonable level of expression as opposed to that seen at 1000 ng/mL, a concentration recommended by the manufacturer. Cell lines were also tested for the ability of the fusion protein to biotinylate a known interacting protein. TrappC12, another subunit of the TRAPPIII complex, was used as an indicator. As expected, both TrappC12 and BirA*-FLAG-TrappC11 were found as biotinylated proteins after streptavidin affinity purification from lysates of tetracycline-induced cells (Figure 3.2 B). Notably, the biotinylation of

TrappC11 and TrappC12 was maximum when the cells were treated with both biotin and tetracycline. A small amount of biotinylated TrappC12 was detected in the biotin added conditions, which suggests some fusion protein was expressed without induction. These results showed that both inducible cell lines were suitable for BioID analysis.
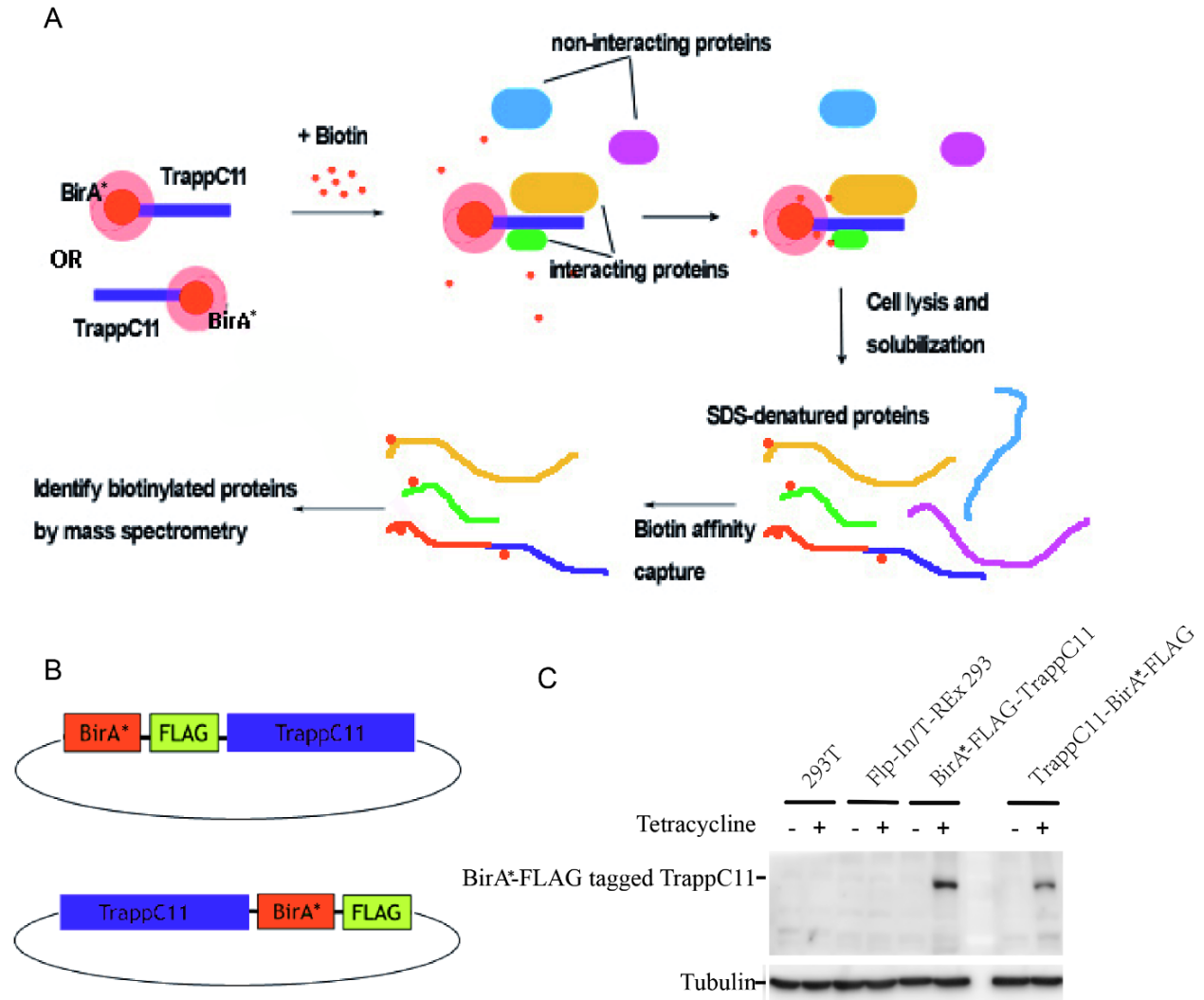
Figure 3.1 Generation of inducible cell lines expressing BirA*-FLAG-tagged TrappC11.
(A) A schematic representation of the BioID method used in this study. (B) Plasmids with different orientations of the BirA*-FLAG tag were used for generating cell lines. (C) Lysates were prepared from 293T, parental Flp-In/T-Rex, BirA*-FLAG-TrappC11, and TrappC11-BirA*-FLAG cells incubated without or with 1000 ng/mL tetracycline overnight as indicated.
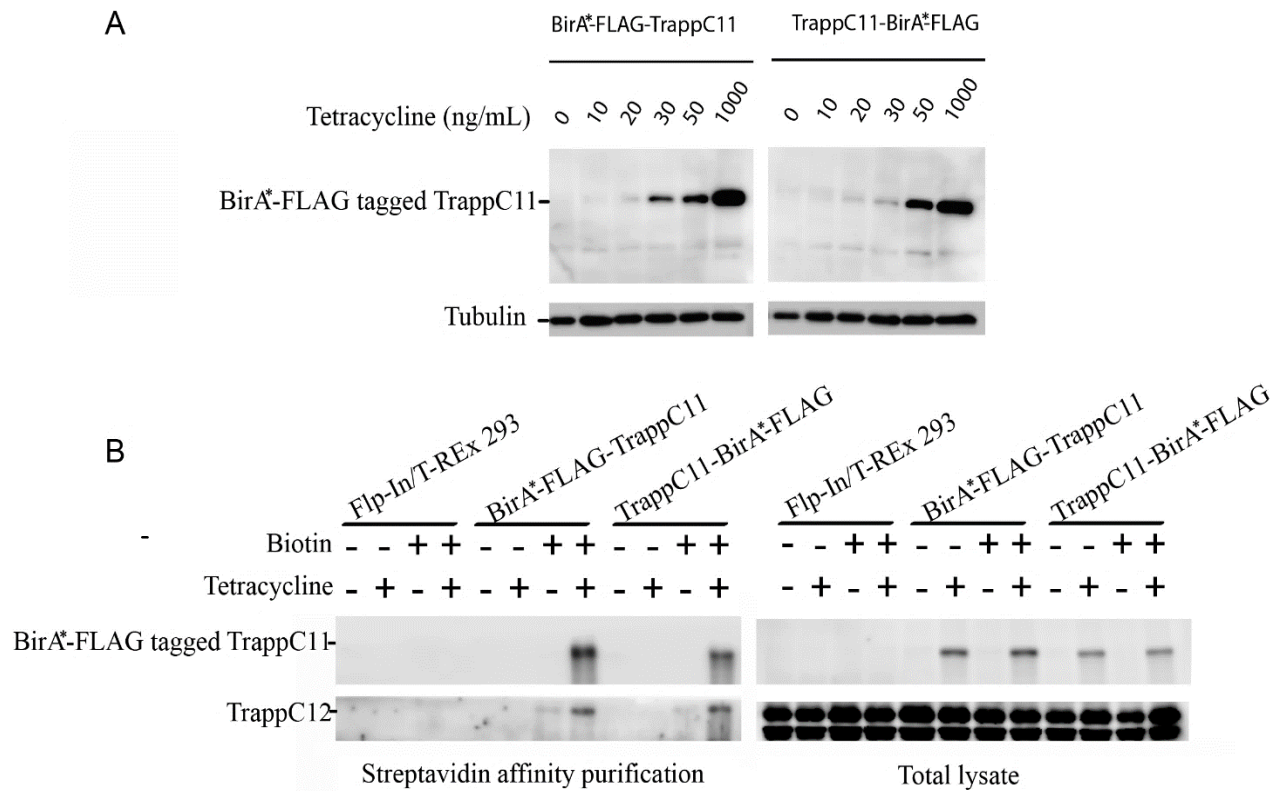
Figure 3.2 TrappC11 BioID cell lines biotinylate TrappC12 within the same complex.
(A) Lysates from two BioID cell lines treated with increasing concentrations of tetracycline were subjected to SDS-PAGE followed by western analysis. Antibody against FLAG was used to analyze expression of the tagged TrappC11. (B) Lysates from BioID cell lines treated with biotin were subjected to streptavidin affinity purification followed by SDS-PAGE. Expression and biotinylation of TrappC12 and tagged TrappC11 were verified by western analysis.

3.2 Mass spectrometry analysis of BioID samples identify TrappC11-interacting proteins.

To identify TrappC11 interacting proteins, biotinylated proteins from induced BirA*-fusion TrappC11 cells and control cells were isolated using streptavidin affinity purification. The control cells were generated using the empty BirA*-FLAG plasmid backbones. The streptavidin affinity purified mixtures were then analyzed by mass spectrometry. In addition to TrappC11 itself, 60 TrappC11-interacting proteins were identified, including 4 other TRAPP subunits: TrappC2L, TrappC8, TrappC12 and TrappC13 (Table 3.1). As expected, identified interacting proteins are involved in different biological processes, with a large portion involved in membrane transport (Figure 3.3). Notably, Sec23IP was identified as an interacting protein, consistent with previously reported immunoprecipitation results (Bassik et al., 2013).

Interestingly, there were 5 identified interacting proteins that play roles in autophagy regulation: ATG2A, ATG2B, WDR45/WIPI-4, SQSTM1/p62, and NBR1. ATG2A and ATG2B are required for both autophagosome formation as well as regulation of lipid droplet morphology and dispersion. (Velikkakath et al., 2012). WDR45/WIPI-4 is a homologue of ATG18 which is suggested to regulate initiation of autophagosome formation (Proikas-Cezanne et al., 2004). SQSTM1/p62 and NBR1 are selective autophagy receptors, playing important roles in cargo recognition in selective autophagy (Zaffagnini and Martens, 2016). The identification of the autophagy-related proteins in the TrappC11 interacting pool suggests the involvement of TrappC11 in autophagic regulation.

Table 3.1: Summary of identified TrappC11 interacting proteins

Entry	Gene	Gene full name	Unique peptides* N-term	Unique peptides* C-term
Q96BY7	ATG2B	Autophagy-related protein 2 homolog B	58/4	2/6
O14641	DVL2	Segment polarity protein dishevelled homolog DVL-2	11/3	5/3
Q641Q2	FAM21A	WASH complex subunit FAM21A	11/1	0/2
Q9Y6Y8	SEC23IP	SEC23-interacting protein	11/0	10/0
Q9Y4E1	FAM21C	WASH complex subunit FAM21C	10/1	0/1
Q6ZTW0	TPGS1	Tubulin polyglutamylase complex subunit 1	10/3	1/4
Q9Y484	WDR45	WD repeat domain phosphoinositide-interacting protein 4	10/0	1/0
Q96JB2	COG3	Conserved oligomeric Golgi complex subunit 3	9/0	0/0
Q8WVT3	TRAPPC12	protein particle complex subunit 12	8/0	12/0
O60566	BUB1B	Mitotic checkpoint serine/threonine-protein kinase BUB1 beta	7/2	0/1
P27708	CAD	CAD protein	7/0	8/0
Q8TDM6	DLG5	Disks large homolog 5	7/0	1/0
O75665.3	OFD1	Oral-facial-digital syndrome 1 protein	7/1	0/1
Q13625	TP53BP2	Apoptosis-stimulating of p53 protein 2	7/1	0/0
30419.2	NMT1	Glycylpeptide N-tetradecanoyltransferase 1	6/0	0/0
Q9H6T3	RPAP3	RNA polymerase II-associated protein 3	6/1	1/0
Q96C92	SDCCAG3	Serologically defined colon cancer antigen 3	6/1	1/2
Q9UPQ9	TNRC6B	Trinucleotide repeat-containing gene 6B protein	6/1	0/0
Q9Y2L5	TRAPPC8	Trafficking protein particle complex subunit 8	6/0	19/0
Q9UL33	TRAPPC2L	Trafficking protein particle complex subunit 2-like protein	5/0	4/0
Q9HB71	CACYBP	Calcyclin-binding protein	4/0	0/0
A6NKD9	CCDC85C	Coiled-coil domain-containing protein 85C	4/1	0/0
Q9UKF6	CPSF3	Cleavage and polyadenylation specificity factor subunit 3	4/1	0/0
Q14126	DSG2	Desmoglein-2	4/1	0/0
P07814	EPRS	Bifunctional glutamate/proline--tRNA ligase	4/2	2/2
P51114	FXR1	Fragile X mental retardation syndrome-related protein 1	4/2	0/0
P35232	PHB	Prohibitin	4/1	2/1
P55036	PSMD4	26S proteasome non-ATPase regulatory subunit 4	4/1	0/1
Q9H6R7	WDCP	WD repeat and coiled-coil-containing protein	4/0	0/0
Q9BRX9	WDR83	WD repeat domain-containing protein 83	4/2	0/2
Q9Y5A9	YTHDF2	YTH domain-containing family protein 2	4/0	1/1
Q7Z739	YTHDF3	YTH domain-containing family protein 3	4/0	1/1
P10398	ARAF	Serine/threonine-protein kinase A-Raf	3/0	3/1
Q9NRA8	EIF4ENIF1	Eukaryotic translation initiation factor 4E transporter	3/1	0/0
Q9NZB2	FAM120A	Constitutive coactivator of PPAR-gamma-like protein 1	3/2	3/1
Q02790	FKBP4	Peptidyl-prolyl cis-trans isomerase FKBP4	3/0	0/0

P51116	FXR2	Fragile X mental retardation syndrome-related protein 2	3/1	0/0
P07195	LDHB	L-lactate dehydrogenase B chain	3/1	1/2
Q9Y5V3	MAGED1	Melanoma-associated antigen D1	3/1	1/1
Q15555	MAPRE2	Microtubule-associated protein RP/EB family member 2	3/1	1/2
Q13765	NACA	Nascent polypeptide-associated complex subunit alpha	3/1	0/2
Q8IVD9	NUDCD3	NudC domain-containing protein 3	3/0	0/0
Q8N1F7	NUP93	Nuclear pore complex protein Nup93	3/2	3/3
Q01968	OCRL	Inositol polyphosphate 5-phosphatase OCRL-1	3/1	0/0
Q13501	SQSTM1	Sequestosome-1	3/0	0/0
Q9UHD2	TBK1	Serine/threonine-protein kinase TBK1	3/0	0/1
P23258	TUBG1	Tubulin gamma-1 chain	3/1	4/4
P01023	A2M	Alpha-2-macroglobulin	2/1	2/0
Q2TAZ0	ATG2A	Autophagy-related protein 2 homolog A	2/0	0/0
Q63ZY3	KANK2	KN motif and ankyrin repeat domain-containing protein 2	2/0	0/1
Q99707	MTR	Methionine synthase	2/0	0/0
Q14596	NBR1	Next to BRCA1 gene 1 protein	2/0	0/1
O60551	NMT2	Glycylpeptide N-tetradecanoyltransferase 2	2/0	0/0
P11216	PYGB	Glycogen phosphorylase, brain form	2/0	0/0
O95486	SEC24A	Protein transport protein Sec24A	2/0	0/0
O94979.7	SEC31A	Protein transport protein Sec31A	2/0	0/0
P50225	SULT1A1	Sulfotransferase 1A1	2/0	0/2
Q6UB35	MTHFD1L	Monofunctional C1-tetrahydrofolate synthase, mitochondrial	1/1	5/2
P30101	PDIA3	Protein disulfide-isomerase A3	1/0	2/0
A5PLN9	TRAPPC13	Trafficking protein particle complex subunit 13	0/0	11/0

The unique peptides number of TrappC11 expression cells / control cells are presented for both orientations of BirA-FLAG tags.
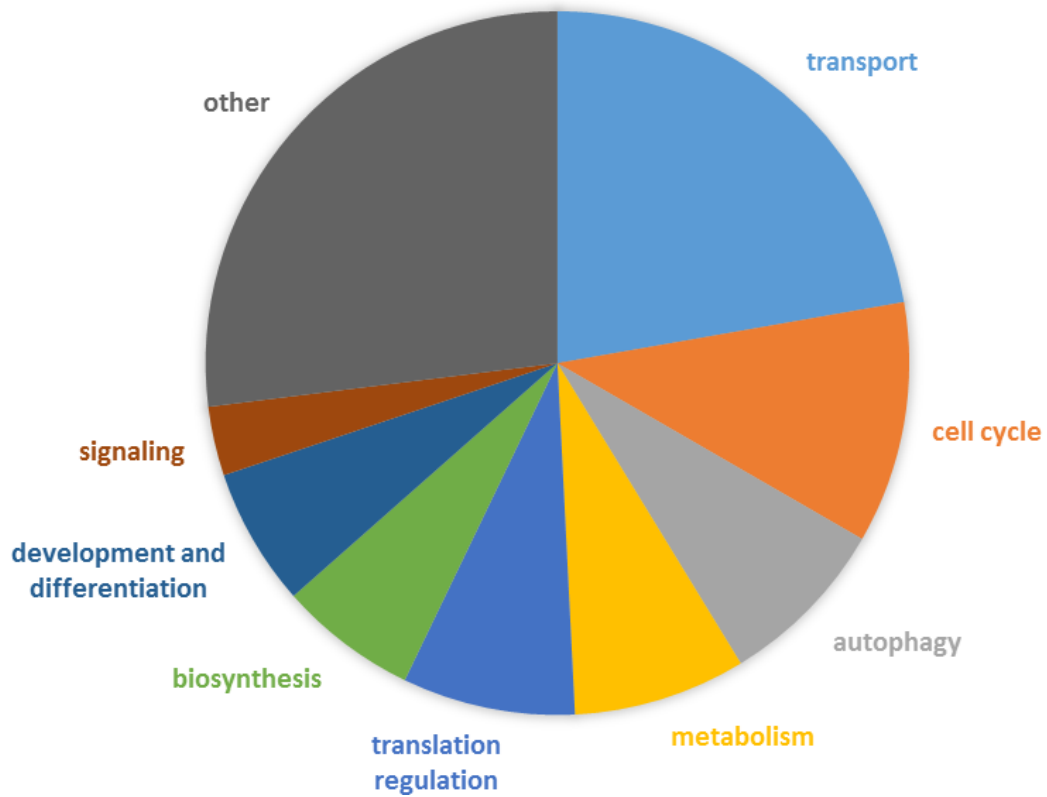
Figure 3.3 The contribution of TrappC11 interacting proteins in different cellular processes.
The identified TrappC11 interacting proteins were categorized based on their functions listed in
the UniProt database.

3.3 TrappC11 RNAi treatment leads to a block in autophagic flux

As indicated by the identified TrappC11 interacting proteins, TrappC11 might play a role in autophagy through interacting with other autophagy regulatory proteins. To study the function of TrappC11 in autophagy, TrappC11 was depleted by siRNA treatment (Figure 3.4). Interestingly, the level of LC3-II, the marker protein for autophagosomes, increased in TrappC11 knockdown cells even in nutrient rich conditions. Compared to untreated HeLa cells in which LC3-II level increased at 1 hour starvation and then decreased, TrappC11 knockdown cells did not show the initial increase in LC3-II. Bafilomycin is a small molecule that blocks autophagosome-lysosome fusion which can result in an increase in LC3-II levels. When control HeLa cells and TrappC11 knockdown cells were treated with bafilomycin, the control cells showed a larger increase in LC3-II level compared to the knockdown cells. This suggests a role for TrappC11 in autophagosome-lysosome fusion prior to starvation. The accumulation of autophagosomes in nutrient rich TrappC11 knockdown cells was also observed in a HeLa cell line expressing GFP-tagged LC3 (Figure 3.5). The number of autophagosomes in non-starved TrappC11 knockdown cells is two-fold higher compared to control cells, while in the other two conditions the autophagosome numbers did not show a noticeable difference.
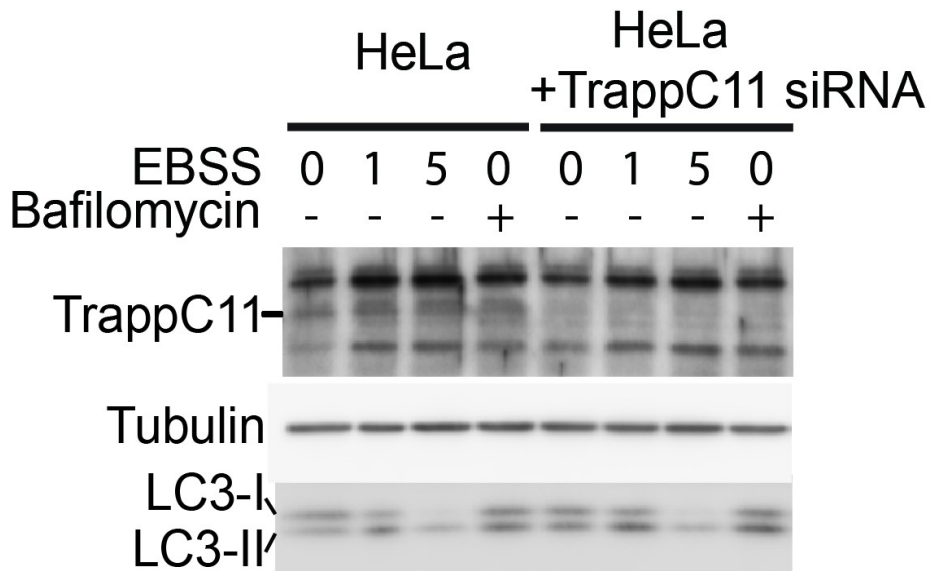
Figure 3.4 Depletion of TrappC11 by siRNA increases LC3-II levels.

HeLa cells were treated without or with siRNA against TrappC11 twice for 5 days before starvation treatments with EBSS. For bafilomycin treatment, cells were cultured in complete medium with 200 nM bafilomycin for 5 hours before collection.
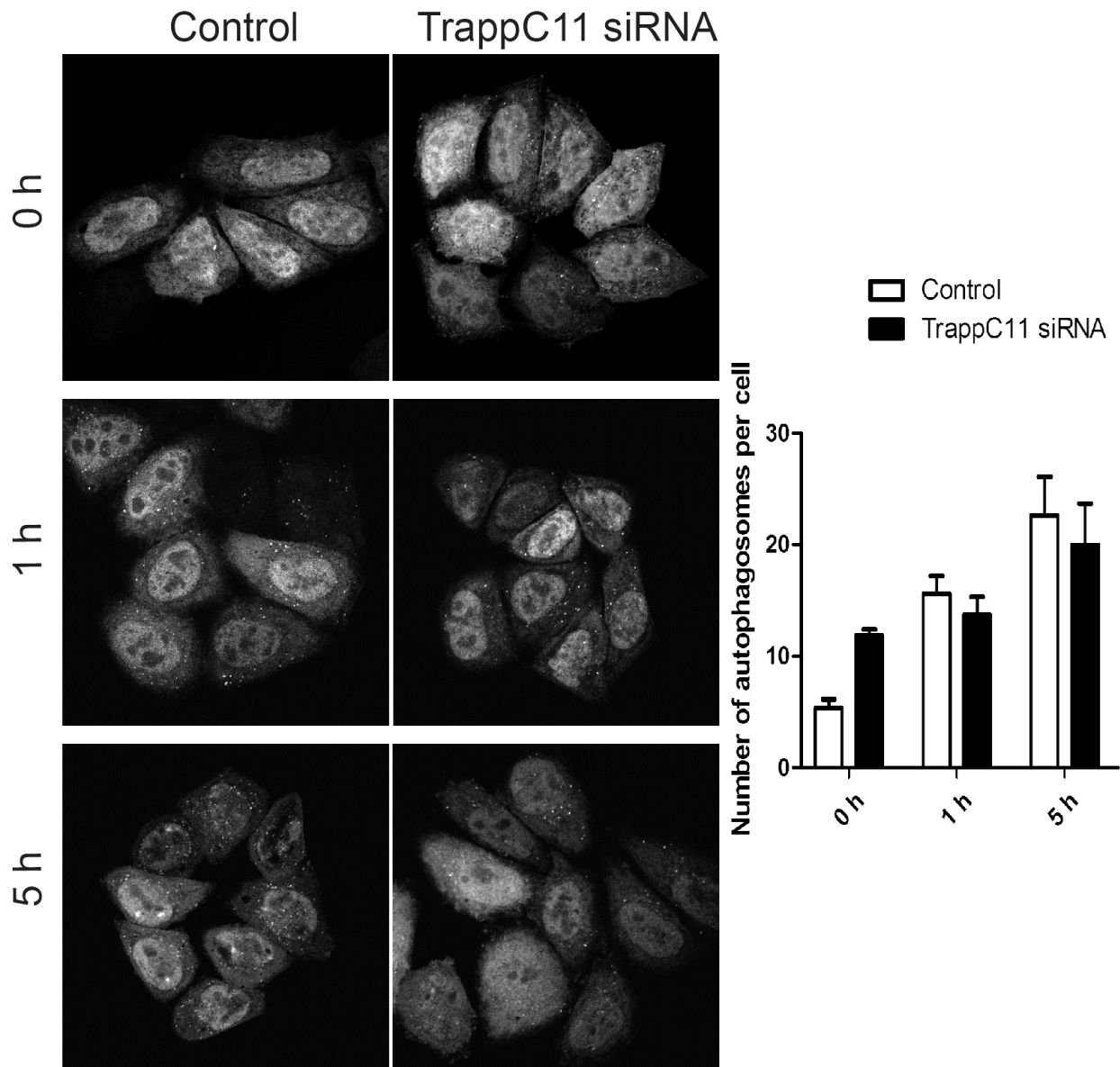
Figure 3.5 Depletion of TrappC11 increases the number of autophagosomes before starvation. HeLa cell line expressing GFP-RFP-LC3 was treated without or with siRNA against TrappC11 twice for 5 days. For starvation conditions, cells were washed with PBS three times following incubation in EBSS for 1 hour or 5 hours before fixation. Images show the GFP signal. Numbers of autophagosomes of each cell were counted in 6 different fields from 2 individual experiments.

3.4 TrappC11 mutated cells generated by CRISPR/Cas9 show defective autophagy

To avoid the possible stress introduced by transfection of the siRNA when studying the function of TrappC11 on autophagy, I used CRISPR/Cas9 to generate a stable TrappC11 null cell line. Unfortunately, from 80 monoclonal cell lines I obtained after transfection with CRISPR RNA complex, only one (#58) showed decreased TrappC11 expression (Figure 3.6 A). This cell line was used as a stable TrappC11 knockdown cell line for further studies. In the starvation experiments performed with HeLa and stable TrappC11 knockdown cells, the knockdown cells showed significant accumulation of LC3-II in nutrient rich conditions (Figure 3.6 B). Compared to the parental HeLa cells, LC3-II levels remained elevated in the starvation conditions, although they showed a tendency to decrease after starvation.

The staining of endogenous LC3 also showed accumulation of LC3 puncta in the nutrient rich conditions of the stable TrappC11 knockdown cells and TrappC11 siRNA treated cells compared to the parental HeLa cells (Figure 3.7). Consistent with the GFP-RFP-LC3 cell line, a difference in the number of LC3-positive puncta was not observed between starved TrappC11 knockdown cells and the parental HeLa cells.
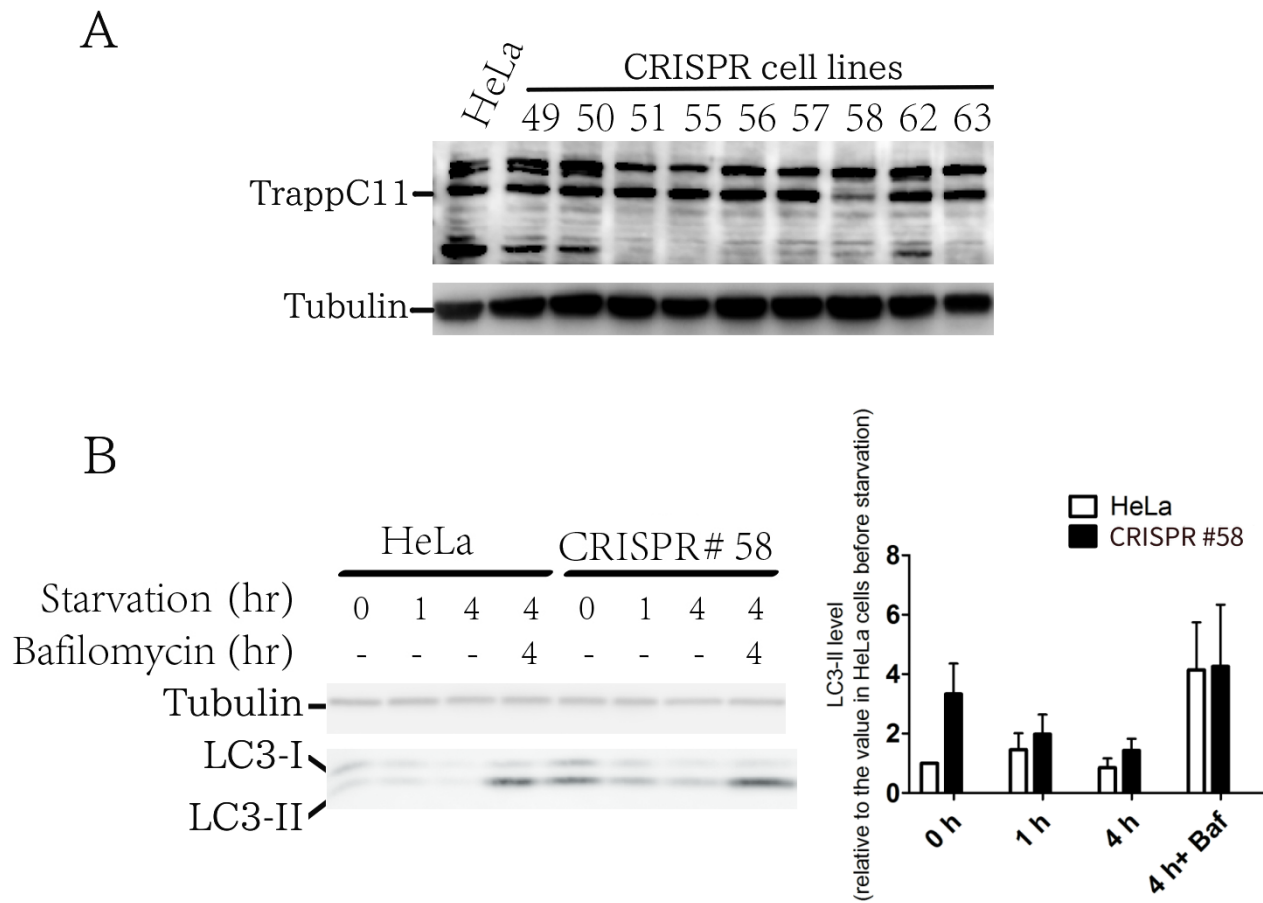
Figure 3.6 TrappC11 knockdown cell line generated through CRISPR/Cas9 shows increased LC-II expression.

(A) Number 58 cell line generated through CRISPR/Cas9 expressed less TrappC11 compared to HeLa and other cell lines. (B) Except for non-starved cells, HeLa cells or stable TrappC11 knockdown cells were washed with PBS three times following incubation in EBSS for 1 hour or 4 hours before lysis. 200 nM bafilomycin was added in EBSS as indicated. The statistics were performed through signal intensity measurement in ImageJ. Endogenous LC3-II levels are normalized to tubulin and expressed as a ratio of levels in non-starved control HeLa cells. Data were collected from 3 individual experiments.
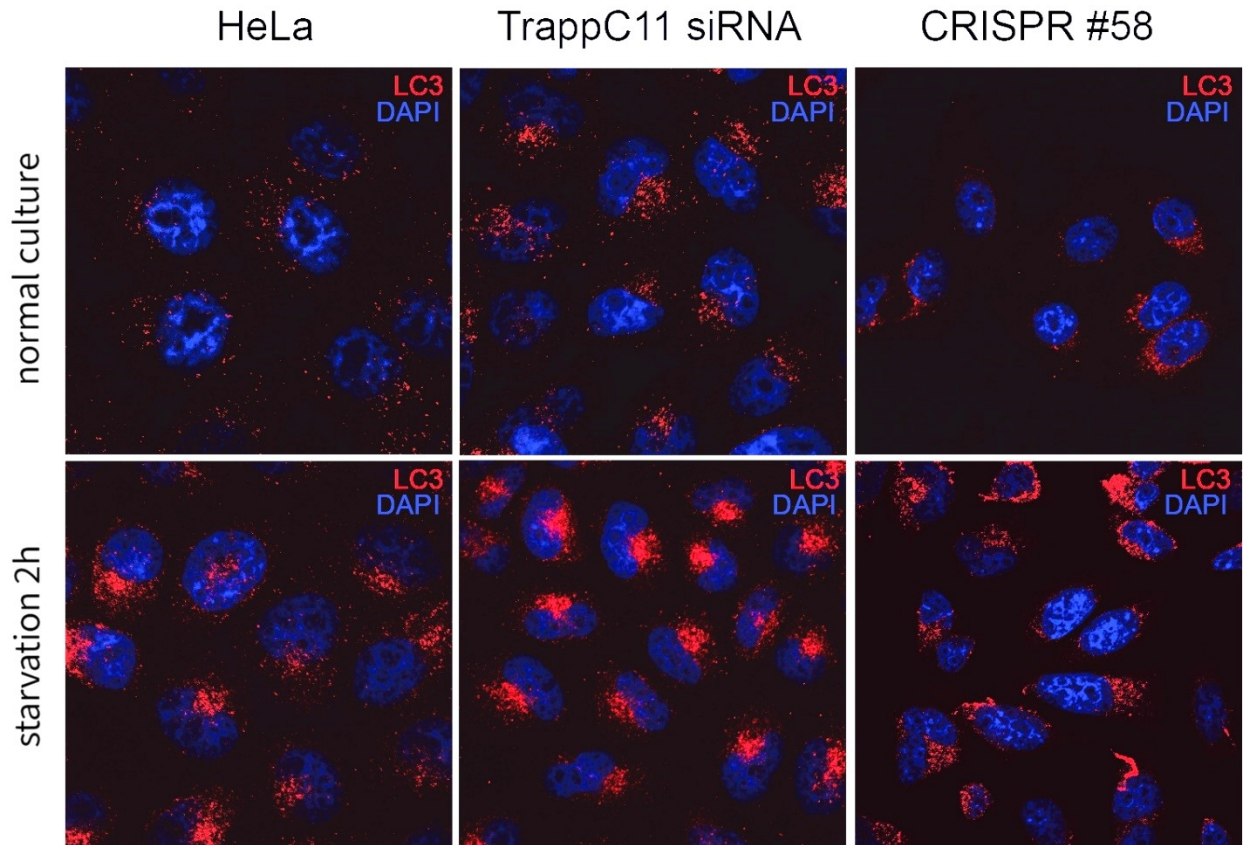
Figure 3.7 Disruption of TrappC11 results in an accumulation of LC3-positive autophagosomes.
Stable TrappC11 knockdown HeLa cells and HeLa cells treated with or without siRNA against TrappC11 were replated on coverslips one day before experiments and fixation. For starvation conditions, cells were washed with PBS three times following incubation in EBSS for 2 hours before fixation. Immunofluorescent staining of endogenous LC3 was employed to show autophagosomes.

3.5 The depletion of TrappC11 changes the distribution of lysosomes

As indicated by the western blotting results shown above (Figure 3.4), the accumulation of autophagosomes in nutrient rich conditions could be due to inhibition of fusion between autophagosomes and lysosomes. To further explore the role of TrappC11 in autophagic turnover, I treated HeLa cells with siRNA against TrappC11 and stained for LAMP-1 to examine the distribution of lysosomes. As reported previously, the TrappC11 knockdown dispersed the Golgi apparatus as indicated by staining for the Golgi marker protein p115. This dispersed Golgi is a good indicator that TrappC11 knockdown was efficient. Interestingly, the result suggests that when TrappC11 levels are reduced, more cells showed lysosomes in a perinuclear region compared to control (Figure 3.8).
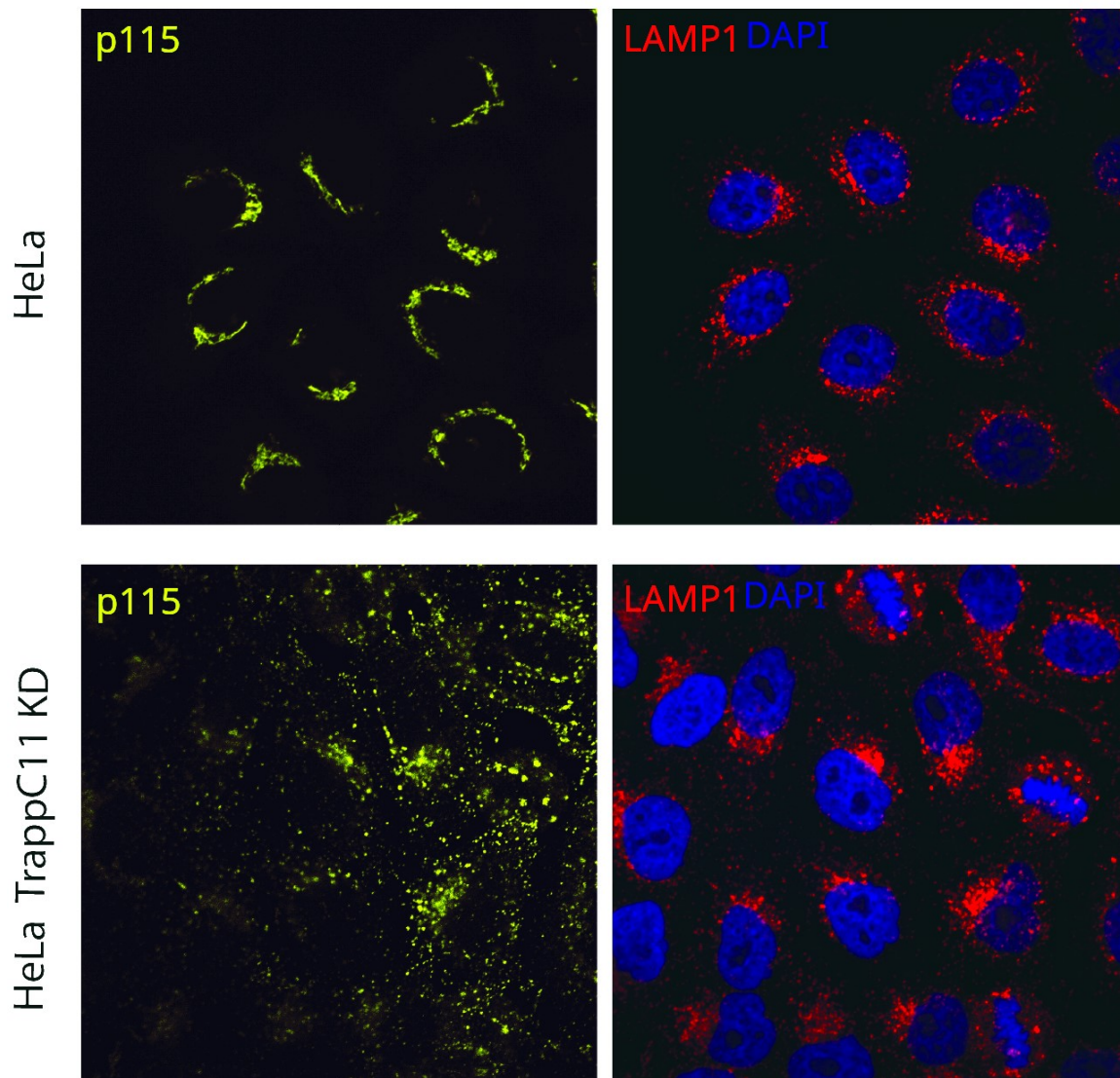
Figure 3.8 Depletion of TrappC11 changes the localization of lysosomes.

HeLa cells were plated on coverslips and treated with or without siRNA against TrappC11 for 3 days. Immunofluorescent staining of p115 and LAMP1 was employed to show Golgi and lysosomes, respectively.

3.6 TrappC11 is important for lipid homeostasis

Considering the lipid accumulation in *TRAPPC11* mutant zebrafish liver and patient fibroblasts, I considered whether knockdown of TrappC11 could mimic this phenotype. Indeed, accumulated lipid droplets were found in both TrappC11 knockdown cells and *TRAPPC11* mutant cells (Figure 3.9). Compared to normal HeLa cells, cells expressing less TrappC11 contained lipid droplets with a significant elevation in both their number and size.
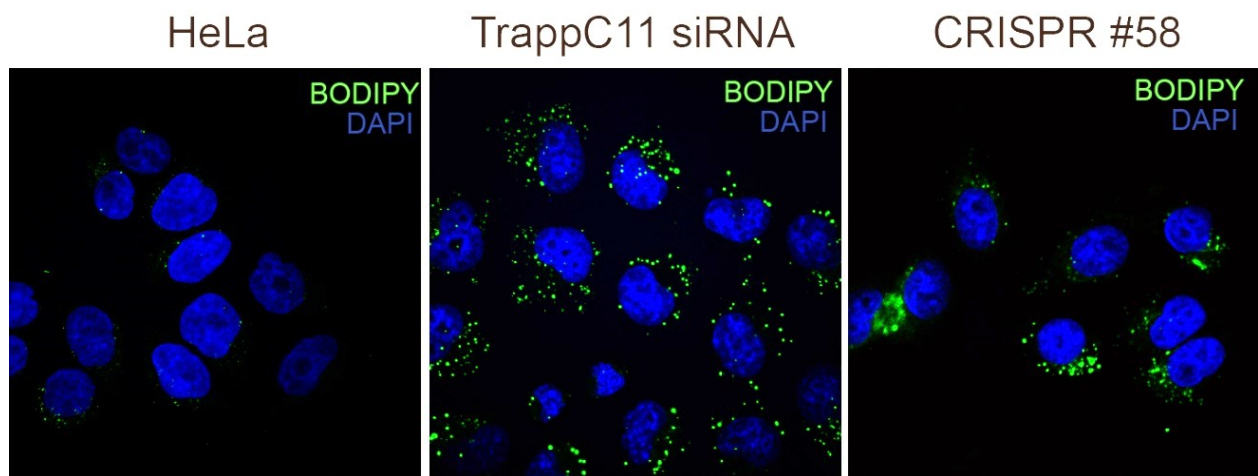
Figure 3.9 Disruption of TrappC11 leads to an accumulation of lipid droplets.
Stable TrappC11 knockdown HeLa cells and HeLa cells treated with or without siRNA against TrappC11 were replated on coverslips and cultured in normal cultural medium. Cells were then fixed with 4% PFA and stained with BODIPY to reveal the lipid droplets.

3.7 Localization of TrappC11-eGFP

To visualize the interaction between TrappC11 and autophagy regulatory proteins, I constructed a plasmid expressing TrappC11 tagged with eGFP (eGFP-TrappC11) and expressed the protein in mammalian cells. As shown in the transfected HeLa cells, eGFP-TrappC11 expressed mostly in the cytoplasm with a concentrated region and a few puncta. The concentrated expression region overlapped with the staining of the Golgi marker proteins p115, mannosidase II (ManII) and GM130.

Considering the interactions between TrappC11 and p62/SQSTM1 suggested by mass spectrometry, I examined whether the eGFP-TrappC11 puncta overlapped with p62/SQSTM. By staining with endogenous p62/SQSTM in eGFP-TrappC11 transfected HeLa cells, I observed partial overlap between p62 puncta and eGFP-TrappC11 puncta (Figure 3.11). Notably, the overlap was absent between eGFP-TrappC11 and LC3 puncta, which is consistent with the mass spectrometry results.
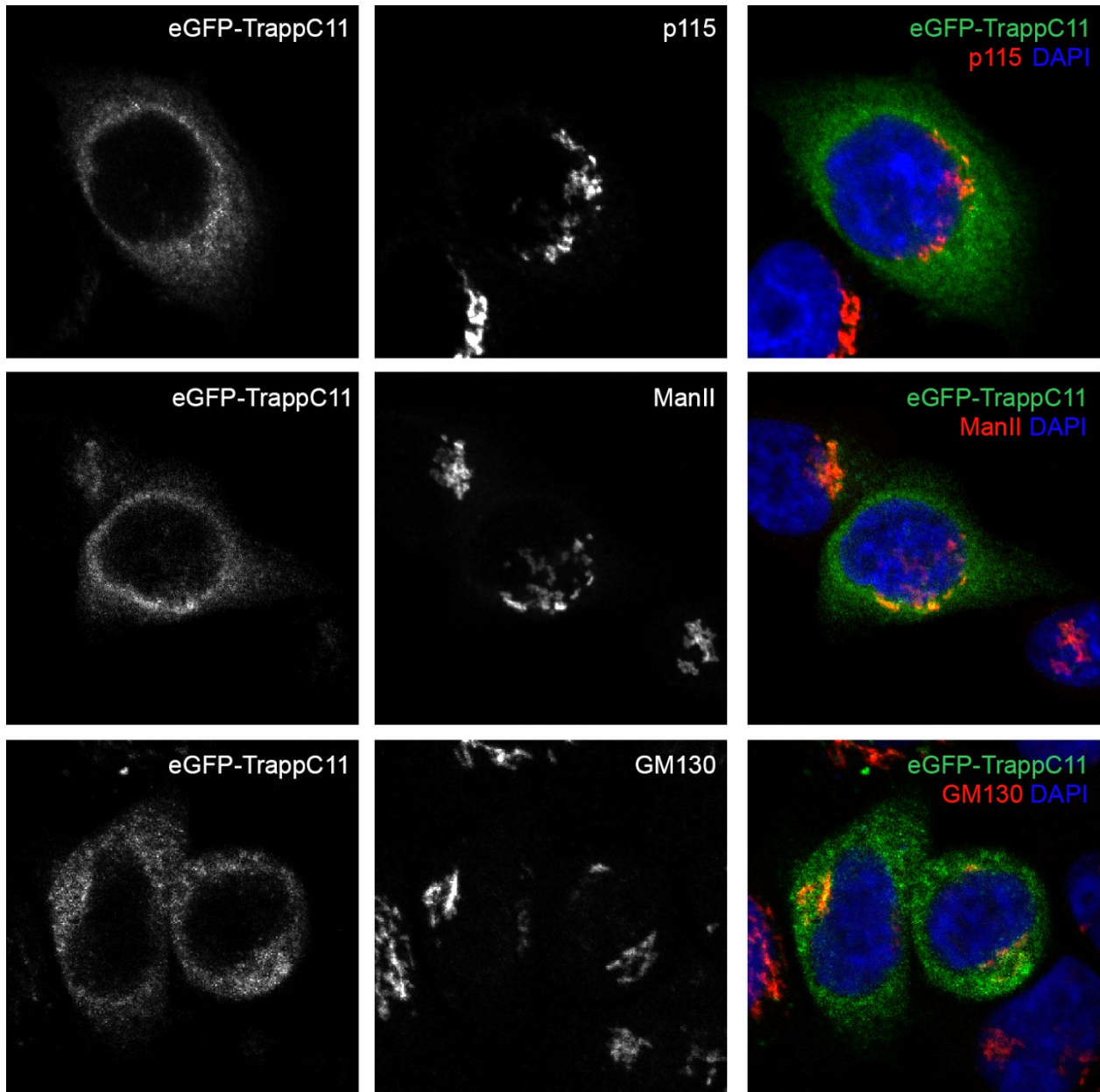
Figure 3.10 eGFP-TrappC11 shows a predominantly cytosolic expression.
HeLa cells were plated on coverslips and transfected with the eGFP-TrappC11 plasmid for 24 hours. Cells were fixed with 4% PFA and stained for p115, ManII or GM130 to show the Golgi.
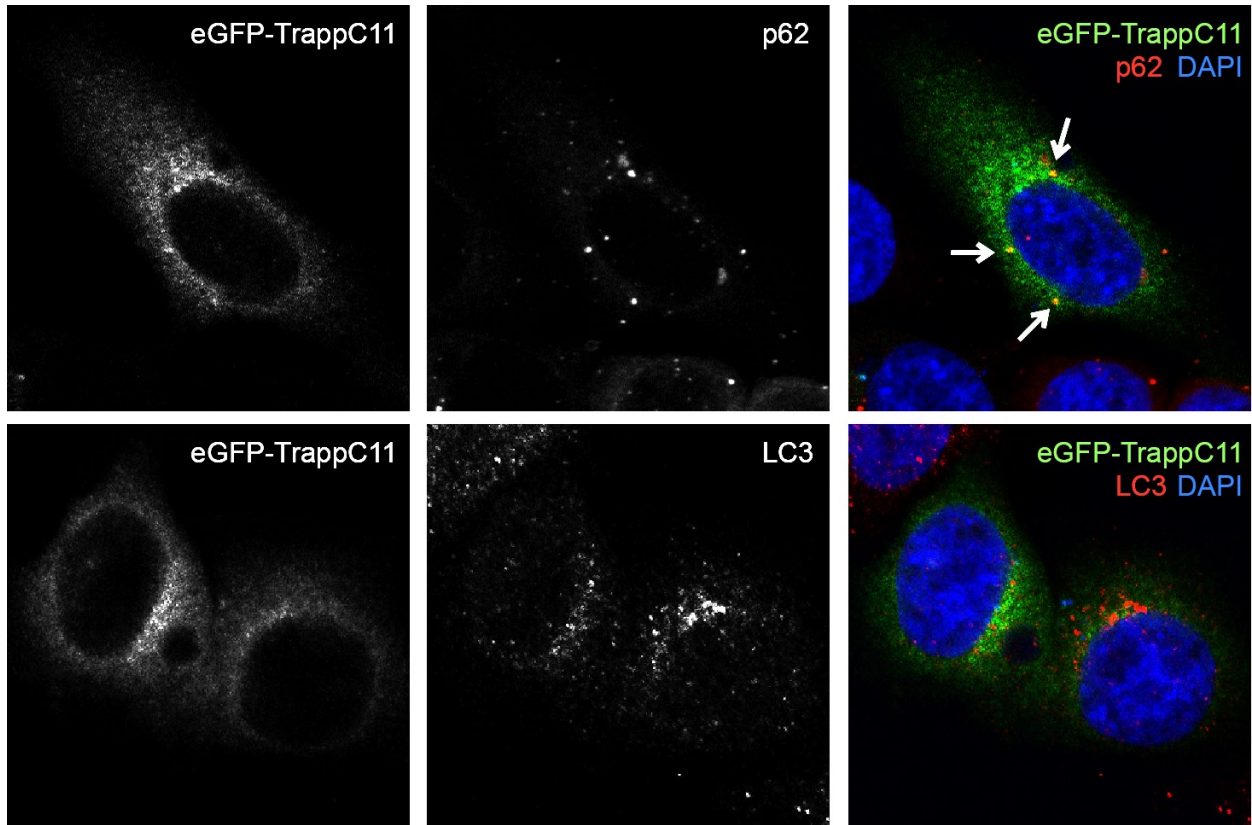
Figure 3.11 eGFP-TrappC11 partially overlaps with p62 but not LC3.

HeLa cells were plated on coverslips and transfected with the eGFP-TrappC11 plasmid for 24 hours. Cells were then fixed with 4% PFA and stained for p62/SQSTM1 and LC3.

Chapter 4: Discussion

As an important cellular quality control mechanism, defects in autophagy lead to a broad range of diseases. For instance, Parkinson's disease, a neurodegenerative disease, is associated with impaired degradation of damaged mitochondria through selective autophagy (Kitada et al., 1998; Matsuda et al., 2010; Valente et al., 2004; Winklhofer and Haass, 2010). Cancer is another disease associated with autophagy. Mutations in ATG2B, ATG5, ATG7, ATG9B, and Beclin which all lead to suppressed autophagy, have been shown to stimulate tumorigenesis (Aita et al., 1999; An et al., 2011; Kang et al., 2009; Liang et al., 1999; Takamura et al., 2011), while autophagy improves cell survival and facilitates tumor cell growth at a later stage of tumor progression (Guo et al., 2013; Yang et al., 2011).

Autophagy also plays a role in maintaining skeletal muscle health and function. Studies have linked reduced autophagy activity with muscle weakness and degeneration. Muscle-specific knockout of the *ATG7* gene in mice leads to sarcomere disorganization and myofiber degeneration resulting from accumulated polyubiquitinated proteins, activated unfolded protein response, and increased damaged mitochondria (Masiero et al., 2009). In fact, autophagy dysfunction has been associated with Duchenne muscular dystrophy (DMD), a severe inherited muscle disorder. Reduced levels of LC3B and elevated accumulation of p62/SQSTM1 were found in muscle samples from both DMD mouse models and patients (Bibee et al., 2014; De Palma et al., 2012). It is likely that the impaired autophagy fails to remove the damaged proteins and organelles, which further leads to the muscular dystrophy.

Notably, patients carrying *TRAPPC11* mutations are reported to have limb girdle or congenital muscular dystrophy with intellectual disability, while autophagy has clear relations with

muscular dystrophy and neurodegenerative diseases. Moreover, a zebrafish *TRAPPC11* mutant is associated with stressed unfolded protein response (UPR) (DeRossi et al., 2016; Senft and Ronai, 2015), and UPR can be induced by inhibited autophagy. Therefore, it is possible that suppressed autophagy contributes to the muscular dystrophy of *TRAPPC11* patients. The results in this thesis showed the accumulation of LC3 in non-starved TrappC11 depletion cells, which suggests that TrappC11 depletion might hinder the non-starvation induced autophagy. Consistent with this notion, BioID-mass spectrometry identified several proteins required for autophagy. ATG2A, ATG2B, and WDR45/WIPI-4, three proteins identified as TrappC11 interacting proteins in this study, were suggested to be required for autophagosome formation. Depletion of ATG2A and B led to the generation of unsealed autophagosomes which suppressed the fusion with lysosomes and caused the accumulation of autophagosomes (Velikkakath et al., 2012). WIPIs, the mammalian orthologues of Atg18, are required for the recruitment of the ATG12 complex, which stimulates membrane expansion of the isolation membrane (Dooley et al., 2014). Notably, TrappC11 depletion also caused the accumulation of autophagosomes before starvation, and the failure of an additive effect by bafilomycin treatment suggests that TrappC11 knockdown could influence the fusion between autophagosomes and lysosomes. Therefore, it would be interesting to understand if the interactions between TrappC11 and ATG2A and B and/or WDR45/WIPI-4 contribute to autophagosome formation.

Another direction worth exploring is the similar effects on lipid droplet accumulation after knockdown of TrappC11 and ATG2. The ATG2 proteins have been shown to be important for lipid droplet morphology and dispersion. They were found on the surface of lipid droplets, and depletion of ATG2s led to an accumulation of cellular lipid droplets (Velikkakath et al., 2012). As shown in this study and previous work (DeRossi et al., 2016; Sadler et al., 2005), TrappC11

depletion or mutation could result in cellular lipid droplet accumulation and fatty liver phenotype. Whether the accumulation of lipid droplets in TrappC11 depleted cells is related to the disruption of the interaction between TrappC11 and ATG2s remains unknown. It would also be interesting to unveil the role of the interaction between TrappC11 and ATG2s in the lipophagy pathway.

To further understand the role of TrappC11 in lipophagy and non-starvation induced autophagy, the interactions between TrappC11 and selective autophagy receptors such as p62/SQSTM1 and NBR1 would be important. The interactions between these two receptors and TrappC11 were discovered by BioID-mass spectrometry, and the colocalization of p62/SQSTM1 and eGFP-TrappC11 was also observed through immunofluorescence microscopy. The interaction between TrappC11 and selective autophagy receptors might stimulate local autophagosome formation and achieve the clearance of specific cargos, such as lipid droplets. However, to understand whether the accumulation of lipid droplets in TrappC11 disrupted cells is due to a failure of recruitment of autophagy receptors requires further investigation.

Studying TRAPPIII complex dependent and independent functions of TrappC11 would also be shed light on the role of TrappC11. TrappC8, another TRAPPIII subunit, was reported to mediate the interaction between TRAPPIII and TBC1D14, which further regulates ATG9 trafficking (Lamb et al., 2016). In contrast to the phenotype after TrappC8 depletion, which has a reduced number of autophagosomes, the results in this thesis showed an increased number of autophagosomes following TrappC11 knockdown. This discrepancy suggests the possibility that TrappC11 could have a TRAPIII-independent role in autophagy. TrappC11 is the only known TRAPP subunit related to lipid homeostasis, which also indicates its possible TRAPPIII-independent function. Future studies to clarify if other subunits in TRAPPIII have similar

autophagy-related phenotypes as TrappC11 should lead to a better understanding of the relation between TrappC11 and the TRAPPIII complex.

As a large, multiple-domain protein, TrappC11 might have multiple functions corresponding to different regions. As shown by the BioID-mass spectrometry results, some interactions only occurred when TrappC11 was tagged at a particular terminus. Except for TrappC13, all the TRAPP subunits as well as some trafficking proteins found as interacting proteins were biotinylated by the BirA*-fused TrappC11 in both orientations, while most proteins only biotinylated with N-terminal tagged TrappC11, and a few only biotinylated with C-terminal tagged TrappC11. All autophagy-related proteins identified in this study were only found with N-terminal tagged TrappC11. Considering the relatively large size of BirA*, there could be a potential disruption of the normal function of the tagged terminus of TrappC11. Therefore, the binding to other subunits and formation of the TRAPPIII complex might not require the function of either terminus, while the interaction with autophagy-related proteins might require the functional C-terminus of TrappC11. On the other hand, the *TRAPPC11* patients have all been reported to have functional first 100 amino acids and the attempt to generate TrappC11 knockout cells by introducing a frame shift in exon 2 (aa 1-68) failed in this study. The evidence, thus, suggests the N-terminus of TrappC11 is required for viability. Therefore, rather than a TrappC11 knockout, generating cells expressing various mutant forms of TrappC11 and mapping functional domains might be a better approach for studying the role of TrappC11 in autophagy as well as other processes.

It is clear that TrappC11 has important roles in the secretory pathway (DeRossi et al., 2016; Scrivens et al., 2011), and the growing evidence suggests that TrappC11 is also involved in autophagy. However, whether the secretory function of TrappC11 relates to its autophagy function

remains unknown. Exploring of the functions of TrappC11 might help understand the interplay of the secretory pathway and autophagy. In addition, elucidation of the function of TrappC11 in autophagy could help explain the development of the disease phenotypes in TrappC11 mutants and contribute to the design of treatments.

References

Aita, V. M., Liang, X. H., Murty, V. V, Pincus, D. L., Yu, W., Cayanis, E., … Levine, B. (1999). Cloning and genomic organization of beclin 1, a candidate tumor suppressor gene on chromosome 17q21. *Genomics*, *59*(1), 59–65. https://doi.org/10.1006/geno.1999.5851

An, C. H., Kim, M. S., Yoo, N. J., Park, S. W., & Lee, S. H. (2011). Mutational and expressional analyses of ATG5, an autophagy-related gene, in gastrointestinal cancers. *Pathology, Research and Practice*, *207*(7), 433–7. https://doi.org/10.1016/j.prp.2011.05.002

Axe, E. L., Walker, S. A., Manifava, M., Chandra, P., Roderick, H. L., Habermann, A., … Ktistakis, N. T. (2008). Autophagosome formation from membrane compartments enriched in phosphatidylinositol 3-phosphate and dynamically connected to the endoplasmic reticulum. *The Journal of Cell Biology*, *182*(4), 685–701. https://doi.org/10.1083/jcb.200803137

Badadani, M., & Badadani, M. (2012). Autophagy Mechanism, Regulation, Functions, and Disorders. *ISRN Cell Biology*, *2012*, 1–11. https://doi.org/10.5402/2012/927064

Barrowman, J., Bhandari, D., Reinisch, K., & Ferro-Novick, S. (2010). TRAPP complexes in membrane traffic: convergence through a common Rab. *Nature Reviews Molecular Cell Biology*, *11*(11), 759–763. https://doi.org/10.1038/nrm2999

Bassik, M. C., Kampmann, M., Lebbink, R. J., Wang, S., Hein, M. Y., Poser, I., … Weissman, J. S. (2013). A systematic mammalian genetic interaction map reveals pathways underlying ricin susceptibility. *Cell*, *152*(4), 909–22. https://doi.org/10.1016/j.cell.2013.01.030

Beller, M., Thiel, K., Thul, P. J., & Jäckle, H. (2010). Lipid droplets: A dynamic organelle moves into focus. *FEBS Letters*, *584*(11), 2176–2182. https://doi.org/10.1016/j.febslet.2010.03.022

Bibee, K. P., Cheng, Y.-J., Ching, J. K., Marsh, J. N., Li, A. J., Keeling, R. M., … Wickline, S. A. (2014). Rapamycin nanoparticles target defective autophagy in muscular dystrophy to enhance both strength and cardiac function. *FASEB Journal : Official Publication of the Federation of American Societies for Experimental Biology*, *28*(5), 2047–61. https://doi.org/10.1096/fj.13-237388

Blomen, V. A., Májek, P., Jae, L. T., Bigenzahn, J. W., Nieuwenhuis, J., Staring, J., … Bene, F. Del. (2015). Gene essentiality and synthetic lethality in haploid human cells. *Science (New York, N.Y.)*, *350*(6264), 1092–6. https://doi.org/10.1126/science.aac7557

Bögershausen, N., Shahrzad, N., Chong, J. X., von Kleist-Retzow, J.-C., Stanga, D., Li, Y., … Lamont, R. E. (2013). Recessive TRAPPC11 mutations cause a disease spectrum of limb girdle muscular dystrophy and myopathy with movement disorder and intellectual disability. *American Journal of Human Genetics*, *93*(1), 181–90. https://doi.org/10.1016/j.ajhg.2013.05.028

Bröcker, C., Engelbrecht-Vandré, S., Ungermann, C., Bonifacino, J. S., Glick, B. S., Behnia, R., … Wickner, W. (2010). Multisubunit Tethering Complexes and Their Role in Membrane Fusion. *Current Biology*, *20*(21), R943–R952. https://doi.org/10.1016/j.cub.2010.09.015

Brunet, S., & Sacher, M. (2014). in sickness and in health: The role of TRAPP and associated proteins in disease. *Traffic*, *15*(8), 803–818. https://doi.org/10.1111/tra.12183

Burman, C., & Ktistakis, N. T. (2010). Regulation of autophagy by phosphatidylinositol 3-phosphate. *FEBS Letters*, *584*(7), 1302–1312. https://doi.org/10.1016/j.febslet.2010.01.011

Cai, Y., Chin, H. F., Lazarova, D., Menon, S., Fu, C., Cai, H., … Reinisch, K. M. (2008). The Structural Basis for Activation of the Rab Ypt1p by the TRAPP Membrane-Tethering Complexes. *Cell*, *133*(7), 1202–1213. https://doi.org/10.1016/j.cell.2008.04.049

Chang, J.-Y., Lee, M.-H., Lin, S.-R., Yang, L.-Y., Sun, S. H., Sze, C.-I., … Chang, N.-S. (2015). Trafficking protein particle complex 6A delta (TRAPPC6AΔ) is an extracellular plaque-forming protein in the brain. *Oncotarget*, *6*(6), 3578–3589. https://doi.org/10.18632/oncotarget.2876

Chia, P. Z. C., & Gleeson, P. a. (2014). Membrane tethering. *F1000Prime Reports*, *6*(September). https://doi.org/10.12703/P6-74

Chiang, H. L., Terlecky, S. R., Plant, C. P., & Dice, J. F. (1989). A role for a 70-kilodalton heat shock protein in lysosomal degradation of intracellular proteins. *Science*, *246*(4928), 382–385. https://doi.org/10.1126/science.2799391

Cinaroglu, A., Gao, C., Imrie, D., & Sadler, K. C. (2011). Activating transcription factor 6 plays protective and pathological roles in steatosis due to endoplasmic reticulum stress in zebrafish. *Hepatology*, *54*(2), 495–508. https://doi.org/10.1002/hep.24396

Cuervo, A. M., & Dice, J. F. (1996). A Receptor for the Selective Uptake and Degradation of Proteins by Lysosomes. *Science*, *273*(5274), 501–503. https://doi.org/10.1126/science.273.5274.501

De Palma, C., Morisi, F., Cheli, S., Pambianco, S., Cappello, V., Vezzoli, M., … Clementi, E. (2012). Autophagy as a new therapeutic target in Duchenne muscular dystrophy. *Cell Death & Disease*, *3*, e418. https://doi.org/10.1038/cddis.2012.159

DeRossi, C., Vacaru, A., Rafiq, R., Cinaroglu, A., Imrie, D., Nayar, S., … Sadler, K. C. (2016). trappc11 is required for protein glycosylation in zebrafish and humans. *Molecular Biology of the Cell*, *27*(8), 1220–1234. https://doi.org/10.1091/mbc.E15-08-0557

Dice, J. F. (1990). Peptide sequences that target cytosolic proteins for lysosomal proteolysis. *Trends in Biochemical Sciences*, *15*(8), 305–309. https://doi.org/10.1016/0968-0004(90)90019-8

Dooley, H. C., Razi, M., Polson, H. E. J., Girardin, S. E., Wilson, M. I., & Tooze, S. A. (2014). WIPI2 links LC3 conjugation with PI3P, autophagosome formation, and pathogen clearance by recruiting Atg12-5-16L1. *Molecular Cell*, *55*(2), 238–52. https://doi.org/10.1016/j.molcel.2014.05.021

Dubnau, J., Chiang, A.-S., Grady, L., Barditch, J., Gossweiler, S., McNeil, J., … Tully, T. (2003). The staufen/pumilio Pathway Is Involved in Drosophila Long-Term Memory. *Current Biology*, *13*(4), 286–296. https://doi.org/10.1016/S0960-9822(03)00064-2

Dubuke, M. L., & Munson, M. (2016). The Secret Life of Tethers: The Role of Tethering Factors in SNARE Complex Regulation. *Frontiers in Cell and Developmental Biology Front. Cell Dev. Biol*, *4*(4), 423389–42. https://doi.org/10.3389/fcell.2016.00042

Feng, Y., Backues, S. K., Baba, M., Heo, J.-M., Harper, J. W., & Klionsky, D. J. (2016). Phosphorylation of Atg9 regulates movement to the phagophore assembly site and the rate of autophagosome formation. *Autophagy*, *12*(4), 648–658. https://doi.org/10.1080/15548627.2016.1157237

Ge, L., Melville, D., Zhang, M., & Schekman, R. (2013). The ER-Golgi intermediate compartment is a key membrane source for the LC3 lipidation step of autophagosome biogenesis. *eLife*, *2*, e00947. https://doi.org/10.7554/eLife.00947

Gedeon, Á. K., Colley, A., Jamieson, R., Thompson, E. M., Rogers, J., Sillence, D., … Gécz, J. (1999). Identification of the gene (SEDL) causing X-linked spondyloepiphyseal dysplasia tarda. *Nature Genetics*, *22*(4), 400–404. https://doi.org/10.1038/11976

Gillingham, A. K., Tong, A. H. Y., Boone, C., & Munro, S. (2004). The GTPase Arf1p and the ER to Golgi cargo receptor Erv14p cooperate to recruit the golgin Rud3p to the cis-Golgi. *The Journal of Cell Biology*, *167*(2), 281–292. https://doi.org/10.1083/jcb.200407088

Guo, J. Y., Karsli-Uzunbas, G., Mathew, R., Aisner, S. C., Kamphorst, J. J., Strohecker, A. M., … White, E. (2013). Autophagy suppresses progression of K-ras-induced lung tumors to oncocytomas and maintains lipid homeostasis. *Genes & Development*, *27*(13), 1447–61. https://doi.org/10.1101/gad.219642.113

Gutierrez, M. G. (2004). Rab7 is required for the normal progression of the autophagic pathway in mammalian cells. *Journal of Cell Science*, *117*(13), 2687–2697. https://doi.org/10.1242/jcs.01114

Hamasaki, M., Furuta, N., Matsuda, A., Nezu, A., Yamamoto, A., Fujita, N., … Yoshimori, T. (2013). Autophagosomes form at ER–mitochondria contact sites. *Nature*, *495*(7441), 389–393. https://doi.org/10.1038/nature11910

Hamilton, G., Harris, S. E., Davies, G., Liewald, D. C., Tenesa, A., Starr, J. M., … Deary, I. J. (2011). Alzheimer's Disease Genes Are Associated with Measures of Cognitive Ageing in the Lothian Birth Cohorts of 1921 and 1936. *International Journal of Alzheimer's Disease*, *2011*, 1–11. https://doi.org/10.4061/2011/505984

Hart, T., Chandrashekhar, M., Aregger, M., Steinhart, Z., Brown, K. R., MacLeod, G., … Moffat, J. (2015). High-Resolution CRISPR Screens Reveal Fitness Genes and Genotype-Specific Cancer Liabilities. *Cell*, *163*(6), 1515–1526. https://doi.org/10.1016/j.cell.2015.11.015

Hayashi-Nishino, M., Fujita, N., Noda, T., Yamaguchi, A., Yoshimori, T., & Yamamoto, A. (2010). Electron tomography reveals the endoplasmic reticulum as a membrane source for autophagosome formation. *Autophagy*, *6*(2), 301–3. https://doi.org/dx.doi.org/10.4161/auto.6.2.11134

Hosokawa, N., Hara, T., Kaizuka, T., Kishi, C., Takamura, A., Miura, Y., … Mizushima, N. (2009). Nutrient-dependent mTORC1 association with the ULK1-Atg13-FIP200 complex required for autophagy. *Molecular Biology of the Cell*, *20*(7), 1981–91. https://doi.org/10.1091/mbc.E08-12-1248

Ichimura, Y., Kirisako, T., Takao, T., Satomi, Y., Shimonishi, Y., Ishihara, N., … Ohsumi, Y. (2000). A ubiquitin-like system mediates protein lipidation. *Nature*, *408*(6811), 488–92. https://doi.org/10.1038/35044114

Itakura, E., Kishi-Itakura, C., & Mizushima, N. (2012). The hairpin-type tail-anchored SNARE syntaxin 17 targets to autophagosomes for fusion with endosomes/lysosomes. *Cell*, *151*(6), 1256–69. https://doi.org/10.1016/j.cell.2012.11.001

Jahn, R., & Scheller, R. H. (2006). SNAREs — engines for membrane fusion. *Nature Reviews Molecular Cell Biology*, *7*(9), 631–643. https://doi.org/10.1038/nrm2002

Jiang, P., & Mizushima, N. (2013). Autophagy and human diseases. *Nature Publishing Group*, *24*(24), 69–7969. https://doi.org/10.1038/cr.2013.161

Jiang, P., Nishimura, T., Sakamaki, Y., Itakura, E., Hatta, T., Natsume, T., & Mizushima, N. (2014). The HOPS complex mediates autophagosome-lysosome fusion through interaction with syntaxin 17. *Molecular Biology of the Cell*, *25*(8), 1327–1337. https://doi.org/10.1091/mbc.E13-08-0447

Kang, M. R., Kim, M. S., Oh, J. E., Kim, Y. R., Song, S. Y., Kim, S. S., … Lee, S. H. (2009). Frameshift mutations of autophagy-related genes ATG2B, ATG5, ATG9B and ATG12 in gastric and colorectal cancers with microsatellite instability. *The Journal of Pathology*, *217*(5), 702–6. https://doi.org/10.1002/path.2509

Karanasios, E., Stapleton, E., Manifava, M., Kaizuka, T., Mizushima, N., Walker, S. A., … Eskelinen, E.-L. (2013). Dynamic association of the ULK1 complex with omegasomes during autophagy induction. *Journal of Cell Science*, *126*(Pt 22), 5224–38. https://doi.org/10.1242/jcs.132415

Karanasios, E., Stapleton, E., Walker, S. A., Manifava, M., & Ktistakis, N. T. (2013). Live cell imaging of early autophagy events: omegasomes and beyond. *Journal of Visualized Experiments : JoVE*, (77). https://doi.org/10.3791/50484

Kaushik, S., & Cuervo, A. M. (2015). Degradation of lipid droplet-associated proteins by chaperone-mediated autophagy facilitates lipolysis. *Nature Cell Biology*, *17*(6). https://doi.org/10.1038/ncb3166

Kawabata, T., & Yoshimori, T. (2016). Beyond starvation: An update on the autophagic machinery and its functions. *Journal of Molecular and Cellular Cardiology*, *95*, 2–10. https://doi.org/10.1016/j.yjmcc.2015.12.005

Khaminets, A., Behl, C., & Dikic, I. (2016). Ubiquitin-Dependent And Independent Signals In Selective Autophagy. *Trends in Cell Biology*, *26*(1), 6–16. https://doi.org/10.1016/j.tcb.2015.08.010

Kim, J. J., Lipatova, Z., & Segev, N. (2016). TRAPP Complexes in Secretion and Autophagy. *Frontiers in Cell and Developmental Biology*, *4*, 20. https://doi.org/10.3389/fcell.2016.00020

Kim, J., Kundu, M., Viollet, B., & Guan, K.-L. (2011). AMPK and mTOR regulate autophagy through direct phosphorylation of Ulk1. *Nature Cell Biology*, *13*(2), 132–41. https://doi.org/10.1038/ncb2152

Kitada, T., Asakawa, S., Hattori, N., Matsumine, H., Yamamura, Y., Minoshima, S., … Shimizu, N. (1998). Mutations in the parkin gene cause autosomal recessive juvenile parkinsonism. *Nature*, *392*(6676), 605–8. https://doi.org/10.1038/33416

Klionsky, D. J., Abdelmohsen, K., Abe, A., Abedin, M. J., Abeliovich, H., Arozena, A. A., … Zughaier, S. M. (2016). Guidelines for the use and interpretation of assays for monitoring autophagy (3rd edition). *Autophagy*. https://doi.org/10.1080/15548627.2015.1100356

Klionsky, D. J., Cregg, J. M., Dunn, W. A., Emr, S. D., Sakai, Y., Sandoval, I. V, … Ohsumi, Y. (2003). A Unified Nomenclature for Yeast Autophagy-Related Genes. *Developmental Cell*, *5*(4), 539–545. https://doi.org/10.1016/S1534-5807(03)00296-X

Koga, H., Kaushik, S., & Cuervo, A. M. (2010). Altered lipid content inhibits autophagic vesicular fusion. *FASEB Journal : Official Publication of the Federation of American Societies for Experimental Biology*, *24*(8), 3052–65. https://doi.org/10.1096/fj.09-144519

Kraft, C., Deplazes, A., Sohrmann, M., & Peter, M. (2008). Mature ribosomes are selectively degraded upon starvation by an autophagy pathway requiring the Ubp3p/Bre5p ubiquitin protease. *Nature Cell Biology*, *10*(5), 602–10. https://doi.org/10.1038/ncb1723

Kraft, C., Peter, M., & Hofmann, K. (2010). Selective autophagy: ubiquitin-mediated recognition and beyond. *Nature Cell Biology*, *12*(9), 836–841. https://doi.org/10.1038/ncb0910-836

Kümmel, D., Oeckinghaus, A., Wang, C., Krappmann, D., & Heinemann, U. (2008). *Distinct isocomplexes of the TRAPP trafficking factor coexist inside human cells*. *FEBS Letters* (Vol. 582). https://doi.org/10.1016/j.febslet.2008.09.056

Kurusu, T., Koyano, T., Hanamata, S., Kubo, T., Noguchi, Y., Yagi, C., … Kuchitsu, K. (2014). OsATG7 is required for autophagy-dependent lipid metabolism in rice postmeiotic anther development. *Autophagy*, *10*(5), 878–88. https://doi.org/10.4161/auto.28279

Lamb, C. A., Nühlen, S., Judith, D., Frith, D., Snijders, A. P., Behrends, C., & Tooze, S. A. (2016). TBC1D14 regulates autophagy via the TRAPP complex and ATG9 traffic. *The EMBO Journal*, *35*(3), 281–301. https://doi.org/10.15252/embj.201592695

Lapierre, L. R., Gelino, S., Meléndez, A., & Hansen, M. (2011). Autophagy and Lipid Metabolism Coordinately Modulate Life Span in Germline-less C. elegans. *Current Biology*, *21*(18), 1507–1514. https://doi.org/10.1016/j.cub.2011.07.042

Li, W., Li, J., & Bao, J. (2012). Microautophagy: lesser-known self-eating. *Cellular and Molecular Life Sciences*, *69*(7), 1125–1136. https://doi.org/10.1007/s00018-011-0865-5

Liang, W.-C., Zhu, W., Mitsuhashi, S., Noguchi, S., Sacher, M., Ogawa, M., … Nishino, I. (2015). Congenital muscular dystrophy with fatty liver and infantile-onset cataract caused by TRAPPC11 mutations: broadening of the phenotype. *Skeletal Muscle*, *5*, 29. https://doi.org/10.1186/s13395-015-0056-4

Liang, X. H., Jackson, S., Seaman, M., Brown, K., Kempkes, B., Hibshoosh, H., & Levine, B. (1999). Induction of autophagy and inhibition of tumorigenesis by beclin 1. *Nature*, *402*(6762), 672–6. https://doi.org/10.1038/45257

Lipatova, Z., Belogortseva, N., Zhang, X. Q., Kim, J., Taussig, D., & Segev, N. (2012). Regulation of selective autophagy onset by a Ypt/Rab GTPase module. *Proceedings of the National Academy of Sciences of the United States of America*, *109*(18), 6981–6. https://doi.org/10.1073/pnas.1121299109

Lynch-Day, M. A., Bhandari, D., Menon, S., Huang, J., Cai, H., Bartholomew, C. R., … Klionsky, D. J. (2010). Trs85 directs a Ypt1 GEF, TRAPPIII, to the phagophore to promote autophagy. *Proceedings of the National Academy of Sciences*, *107*(17), 7811–7816. https://doi.org/10.1073/pnas.1000063107

Mancias, J. D., & Kimmelman, A. C. (2016). Mechanisms of Selective Autophagy in Normal Physiology and Cancer. *Journal of Molecular Biology*, *428*(9), 1659–1680. https://doi.org/10.1016/j.jmb.2016.02.027

Mancias, J. D., Wang, X., Gygi, S. P., Harper, J. W., & Kimmelman, A. C. (2014). Quantitative proteomics identifies NCOA4 as the cargo receptor mediating ferritinophagy. *Nature*, *509*(7498), 105–9. https://doi.org/10.1038/nature13148

Masiero, E., Agatea, L., Mammucari, C., Blaauw, B., Loro, E., Komatsu, M., … Sandri, M. (2009). Autophagy is required to maintain muscle mass. *Cell Metabolism*, *10*(6), 507–15. https://doi.org/10.1016/j.cmet.2009.10.008

Matsuda, N., Sato, S., Shiba, K., Okatsu, K., Saisho, K., Gautier, C. A., … Tanaka, K. (2010). PINK1 stabilized by mitochondrial depolarization recruits Parkin to damaged mitochondria and activates latent Parkin for mitophagy. *The Journal of Cell Biology*, *189*(2), 211–21. https://doi.org/10.1083/jcb.200910140

Milev, M. P., Hasaj, B., Saint-Dic, D., Snounou, S., Zhao, Q., & Sacher, M. (2015). TRAMM/TrappC12 plays a role in chromosome congression, kinetochore stability, and CENP-E recruitment. *The Journal of Cell Biology*, *209*(2), 221–234. https://doi.org/10.1083/jcb.201501090

Mir, A., Kaufman, L., Noor, A., Motazacker, M. M., Jamil, T., Azam, M., … Vincent, J. B. (2009). Identification of mutations in TRAPPC9, which encodes the NIK- and IKK-beta-binding protein, in nonsyndromic autosomal-recessive mental retardation. *American Journal of Human Genetics*, *85*(6), 909–15. https://doi.org/10.1016/j.ajhg.2009.11.009

Mizushima, N., & Komatsu, M. (2011). Autophagy: Renovation of cells and tissues. *Cell*, *147*(4), 728–741. https://doi.org/10.1016/j.cell.2011.10.026

Mizushima, N., Noda, T., Yoshimori, T., Tanaka, Y., Ishii, T., George, M. D., … Ohsumi, Y. (1998). A protein conjugation system essential for autophagy. *Nature*, *395*(6700), 395–8. https://doi.org/10.1038/26506

Mochida, G. H., Mahajnah, M., Hill, A. D., Basel-Vanagaite, L., Gleason, D., Hill, R. S., … Walsh, C. A. (2009). A truncating mutation of TRAPPC9 is associated with autosomal-recessive intellectual disability and postnatal microcephaly. *American Journal of Human Genetics*, *85*(6), 897–902. https://doi.org/10.1016/j.ajhg.2009.10.027

Morgera, F., Sallah, M. R., Dubuke, M. L., Gandhi, P., Brewer, D. N., Carr, C. M., & Munson, M. (2012). Regulation of exocytosis by the exocyst subunit Sec6 and the SM protein Sec1. *Molecular Biology of the Cell*, *23*(2), 337–46. https://doi.org/10.1091/mbc.E11-08-0670

Nakajima, H. (1991). A cytoskeleton-related gene, uso1, is required for intracellular protein transport in Saccharomyces cerevisiae. *The Journal of Cell Biology*, *113*(2), 245–260. https://doi.org/10.1083/jcb.113.2.245

Popovic, D., Dikic, I., Mizushima, N., Bruns, C., McCaffery, J., Curwin, A., … Alessi, D. (2014). TBC1D5 and the AP2 complex regulate ATG9 trafficking and initiation of autophagy. *EMBO Reports*, *15*(4), 392–401. https://doi.org/10.1002/embr.201337995

Proikas-Cezanne, T., Waddell, S., Gaugel, A., Frickey, T., Lupas, A., & Nordheim, A. (2004). WIPI-1alpha (WIPI49), a member of the novel 7-bladed WIPI protein family, is aberrantly expressed in human cancer and is linked to starvation-induced autophagy. *Oncogene*, *23*(58), 9314–25. https://doi.org/10.1038/sj.onc.1208331

Rabinowitz, J. D., & White, E. (2010). Autophagy and metabolism. *Science (New York, N.Y.)*, *330*(6009), 1344–1348. https://doi.org/10.1126/science.1193497

Reggiori, F., Shintani, T., Chong, H., Nair, U., & Klionsky, D. J. (2005). Atg9 Cycles Between Mitochondria and the Pre-Autophagosomal Structure in Yeasts. *Autophagy*, *1*(2), 101–109. https://doi.org/10.4161/auto.1.2.1840

Reggiori, F., & Tooze, S. A. (2012). Autophagy regulation through Atg9 traffic: Figure 1. *The Journal of Cell Biology*, *198*(2), 151–153. https://doi.org/10.1083/jcb.201206119

Rodriguez-Navarro, J. A., Kaushik, S., Koga, H., Dall'Armi, C., Shui, G., Wenk, M. R., … Cuervo, A. M. (2012). Inhibitory effect of dietary lipids on chaperone-mediated autophagy. *Proceedings of the National Academy of Sciences of the United States of America*, *109*(12), E705-14. https://doi.org/10.1073/pnas.1113036109

Rogov, V., Dötsch, V., Johansen, T., & Kirkin, V. (2014). Interactions between Autophagy Receptors and Ubiquitin-like Proteins Form the Molecular Basis for Selective Autophagy. *Molecular Cell*, *53*(2), 167–178. https://doi.org/10.1016/j.molcel.2013.12.014

Roux, K. J., Kim, D. I., Raida, M., & Burke, B. (2012). A promiscuous biotin ligase fusion protein identifies proximal and interacting proteins in mammalian cells. *Journal of Cell Biology*, *196*(6), 801–810. https://doi.org/10.1083/jcb.201112098

Sacher, M., Barrowman, J., Wang, W., Horecka, J., Zhang, Y., Pypaert, M., & Ferro-Novick, S. (2001). TRAPP I Implicated in the Specificity of Tethering in ER-to-Golgi Transport. *Molecular Cell*, *7*(2), 433–442. https://doi.org/10.1016/S1097-2765(01)00190-3

Sacher, M., Jiang, Y., Barrowman, J., Scarpa, A., Burston, J., Zhang, L., … Ferro-Novick, S. (1998). TRAPP, a highly conserved novel complex on the cis-Golgi that mediates vesicle docking and fusion. *The EMBO Journal*, *17*(9), 2494–2503. https://doi.org/10.1093/emboj/17.9.2494

Sadler, K. C., Amsterdam, A., Soroka, C., Boyer, J., & Hopkins, N. (2005). A genetic screen in zebrafish identifies the mutants vps18, nf2 and foie gras as models of liver disease. *Development (Cambridge, England)*, *132*(15), 3561–3572. https://doi.org/10.1242/dev.01918

Sancak, Y., Peterson, T. R., Shaul, Y. D., Lindquist, R. A., Thoreen, C. C., Bar-Peled, L., & Sabatini, D. M. (2008). The Rag GTPases bind raptor and mediate amino acid signaling to mTORC1. *Science (New York, N.Y.)*, *320*(5882), 1496–501. https://doi.org/10.1126/science.1157535

Scrivens, P. J., Noueihed, B., Shahrzad, N., Hul, S., Brunet, S., & Sacher, M. (2011). C4orf41 and TTC-15 are mammalian TRAPP components with a role at an early stage in ER-to-Golgi trafficking. *Molecular Biology of the Cell*, *22*(12), 2083–2093. https://doi.org/10.1091/mbc.E10-11-0873

Seibenhener, M. L., Babu, J. R., Geetha, T., Wong, H. C., Krishna, N. R., & Wooten, M. W. (2004). Sequestosome 1/p62 is a polyubiquitin chain binding protein involved in ubiquitin proteasome degradation. *Molecular and Cellular Biology*, *24*(18), 8055–68. https://doi.org/10.1128/MCB.24.18.8055-8068.2004

Sekito, T., Kawamata, T., Ichikawa, R., Suzuki, K., & Ohsumi, Y. (2009). Atg17 recruits Atg9 to organize the pre-autophagosomal structure. *Genes to Cells : Devoted to Molecular & Cellular Mechanisms*, *14*(5), 525–38. https://doi.org/10.1111/j.1365-2443.2009.01299.x

Senft, D., & Ronai, Z. A. (2015). UPR, autophagy, and mitochondria crosstalk underlies the ER stress response. *Trends in Biochemical Sciences*, *40*(3), 141–8. https://doi.org/10.1016/j.tibs.2015.01.002

Shalem, O., Sanjana, N. E., Hartenian, E., Shi, X., Scott, D. A., Mikkelsen, T. S., … Joung, J. K. (2014). Genome-scale CRISPR-Cas9 knockout screening in human cells. *Science (New York, N.Y.)*, *343*(6166), 84–7. https://doi.org/10.1126/science.1247005

Shpilka, T., Weidberg, H., Pietrokovski, S., Elazar, Z., Wood, V., Gwilliam, R., … Bateman, A. (2011). Atg8: an autophagy-related ubiquitin-like protein family. *Genome Biology*, *12*(7), 226. https://doi.org/10.1186/gb-2011-12-7-226

Singh, R., Kaushik, S., Wang, Y., Xiang, Y., Novak, I., Komatsu, M., … Czaja, M. J. (2009). Autophagy regulates lipid metabolism. *Nature*, *458*(7242), 1131–1135. https://doi.org/10.1038/nature07976

Spang, A. (2016). Membrane Tethering Complexes in the Endosomal System. *Frontiers in Cell and Developmental Biology Front. Cell Dev. Biol*, *4*(4). https://doi.org/10.3389/fcell.2016.00035

Suzuki, K., Kirisako, T., Kamada, Y., Mizushima, N., Noda, T., & Ohsumi, Y. (2001). The pre-autophagosomal structure organized by concerted functions of APG genes is essential for autophagosome formation. *The EMBO Journal*, *20*(21), 5971–81. https://doi.org/10.1093/emboj/20.21.5971

Sztul, E. (2005). Role of tethering factors in secretory membrane traffic. *AJP: Cell Physiology*, *290*(1), C11–C26. https://doi.org/10.1152/ajpcell.00293.2005

Takamura, A., Komatsu, M., Hara, T., Sakamoto, A., Kishi, C., Waguri, S., … Mizushima, N. (2011). Autophagy-deficient mice develop multiple liver tumors. *Genes & Development*, *25*(8), 795–800. https://doi.org/10.1101/gad.2016211

Taussig, D., Lipatova, Z., & Segev, N. (2014). Trs20 is required for TRAPP III complex assembly at the PAS and its function in autophagy. *Traffic*, *15*(3), 327–337. https://doi.org/10.1111/tra.12145

Valente, E. M., Abou-Sleiman, P. M., Caputo, V., Muqit, M. M. K., Harvey, K., Gispert, S., … Wood, N. W. (2004). Hereditary early-onset Parkinson's disease caused by mutations in PINK1. *Science (New York, N.Y.)*, *304*(5674), 1158–60. https://doi.org/10.1126/science.1096284

van Zutphen, T., Todde, V., de Boer, R., Kreim, M., Hofbauer, H. F., Wolinski, H., … Kohlwein, S. D. (2014). Lipid droplet autophagy in the yeast Saccharomyces cerevisiae. *Molecular Biology of the Cell*, *25*(2), 290–301. https://doi.org/10.1091/mbc.E13-08-0448

Velikkakath, A. K. G., Nishimura, T., Oita, E., Ishihara, N., & Mizushima, N. (2012). Mammalian Atg2 proteins are essential for autophagosome formation and important for regulation of size and distribution of lipid droplets. *Molecular Biology of the Cell*, *23*(5), 896–909. https://doi.org/10.1091/mbc.E11-09-0785

Wang, W., Sacher, M., & Ferro-Novick, S. (2000). Trapp Stimulates Guanine Nucleotide Exchange on Ypt1p. *The Journal of Cell Biology*, *151*(2), 289–296. https://doi.org/10.1083/jcb.151.2.289

Weber, T., Zemelman, B. V, McNew, J. A., Westermann, B., Gmachl, M., Parlati, F., … Rothman, J. E. (1998). SNAREpins: Minimal Machinery for Membrane Fusion. *Cell*, *92*(6), 759–772. https://doi.org/10.1016/S0092-8674(00)81404-X

Wendler, F., Gillingham, A. K., Sinka, R., Rosa-Ferreira, C., Gordon, D. E., Franch-Marro, X., … Trimble, W. (2010). A genome-wide RNA interference screen identifies two novel components of the metazoan secretory pathway. *The EMBO Journal*, *29*(2), 304–314. https://doi.org/10.1038/emboj.2009.350

Weng, Y.-R., Kong, X., Yu, Y.-N., Wang, Y.-C., Hong, J., Zhao, S.-L., & Fang, J.-Y. (2014). The role of ERK2 in colorectal carcinogenesis is partly regulated by TRAPPC4. *Molecular Carcinogenesis*, *53 Suppl 1*, E72-84. https://doi.org/10.1002/mc.22031

Winklhofer, K. F., & Haass, C. (2010). Mitochondrial dysfunction in Parkinson's disease. *Biochimica et Biophysica Acta (BBA) - Molecular Basis of Disease*, *1802*(1), 29–44. https://doi.org/10.1016/j.bbadis.2009.08.013

Yang, L., Li, P., Fu, S., Calay, E. S., & Hotamisligil, G. S. (2010). Defective hepatic autophagy in obesity promotes ER stress and causes insulin resistance. *Cell Metabolism*, *11*(6), 467–78. https://doi.org/10.1016/j.cmet.2010.04.005

Yang, S., Wang, X., Contino, G., Liesa, M., Sahin, E., Ying, H., … Kimmelman, A. C. (2011). Pancreatic cancers require autophagy for tumor growth. *Genes & Development*, *25*(7), 717–29. https://doi.org/10.1101/gad.2016111

Yang, Z., & Klionsky, D. J. (2009). An overview of the molecular mechanism of autophagy. *Current Topics in Microbiology and Immunology*, *335*, 1–32. https://doi.org/10.1007/978-3-642-00302-8_1

Yen, W.-L., Legakis, J. E., Nair, U., & Klionsky, D. J. (2007). Atg27 is required for autophagy-dependent cycling of Atg9. *Molecular Biology of the Cell*, *18*(2), 581–93. https://doi.org/10.1091/mbc.E06-07-0612

Young, A. R. J., Chan, E. Y. W., Hu, X. W., Köchl, R., Crawshaw, S. G., High, S., … Tooze, S. A. (2006). Starvation and ULK1-dependent cycling of mammalian Atg9 between the TGN and endosomes. *Journal of Cell Science*, *119*(Pt 18), 3888–900. https://doi.org/10.1242/jcs.03172

Yu, I.-M., & Hughson, F. M. (2010). Tethering Factors as Organizers of Intracellular Vesicular Traffic. *Annual Review of Cell and Developmental Biology*, *26*(1), 137–156. https://doi.org/10.1146/annurev.cellbio.042308.113327

Zaffagnini, G., & Martens, S. (2016). Mechanisms of Selective Autophagy. *Journal of Molecular Biology*, *428*(9), 1714–1724. https://doi.org/10.1016/j.jmb.2016.02.004

Zhao, S.-L., Hong, J., Xie, Z.-Q., Tang, J.-T., Su, W.-Y., Du, W., … Fang, J.-Y. (2011). TRAPPC4-ERK2 Interaction Activates ERK1/2, Modulates Its Nuclear Localization and Regulates Proliferation and Apoptosis of Colorectal Cancer Cells. *PLoS ONE*, *6*(8), e23262. https://doi.org/10.1371/journal.pone.0023262

Zoncu, R., Bar-Peled, L., Efeyan, A., Wang, S., Sancak, Y., Sabatini, D. M., … Steinberg, B. E. (2011). mTORC1 senses lysosomal amino acids through an inside-out mechanism that requires the vacuolar H(+)-ATPase. *Science (New York, N.Y.)*, *334*(6056), 678–83. https://doi.org/10.1126/science.1207056